Catalysis Science & Technology

ROYAL SOCIETY OF CHEMISTRY

MINI REVIEW

View Article Online
View Journal | View Issue

Check for updates

Cite this: *Catal. Sci. Technol.*, 2020, **10**, 590

Catalysis, kinetics and mechanisms of organo-iridium enantioselective hydrogenation-reduction

Joseph M. Mwansa and Michael I. Page *

Received 24th October 2019,
Accepted 11th December 2019

DOI: 10.1039/c9cy02147g

rsc.li/catalysis

The synthesis of chiral molecules is of great importance to the pharmaceutical, agrochemical, flavour and fragrance industries. The use of organo-iridium complexes has gained a reputation for its great utility in key enantioselective synthetic procedures. Prime examples include the catalytic reduction of carbonyls and imines; iridium-catalysed allylic substitution and catalysed enantioselective hydrogenation of unsaturated carboxylic acids. Important aspects in these processes are the reaction conditions such as the catalyst loading, metal-ion ligands, the substrate, solvent and the reaction times-all of which can affect the degree of enantioselectivity. Understanding the mechanisms of these hydrogenation/reduction reactions through kinetic and other related studies makes a vital contribution to improving catalytic efficiency.

Open Access Article. Published on 11 December 2019. Downloaded on 2/7/2026 6:23:02 AM.
This article is licensed under a Creative Commons Attribution-NonCommercial 3.0 Unported Licence.

1. Introduction

Iridium is an extremely rare element, estimated to be 1 ppb of the Earth's crust and found mainly in Alaska and South Africa as two naturally occurring isotopes. It is the densest element. Its electronic configuration is $[Xe]4f^{14}5d^{7}6s^{2}$ and, as a result of a large crystal field stabilisation energy associated with the t_{2g}^{6} configuration, its most important oxidation state is +3 (d^6). However, the +1 state (d^8), particularly with π-acceptor ligands, and the +4 state (d^5) also occur to a significant extent. Most d^6 complexes are low spin and octahedral with an effective ionic radius for Ir^{3+} of 68 pm. The number of ligand atoms bonded to the iridium is indicated by η followed by a superscript indicating that number of ligand atoms. For example, if the cyclopentadienyl anion ligand bonds through all five atoms, they are designated η^5-C_5H_5. The three most important catalyst classes for enantioselective reactions are neutral iridium(I), cationic iridium(I) and iridium(III).

Many organo-iridium complexes obey the 18-electron rule and are typically "exchange inert". In general ligand exchange occurs by dissociative substitution mechanisms, wherein the rate of reaction is determined by the rate of dissociation of a ligand. Conversely, 18-electron compounds can be highly reactive towards electrophiles such as protons and such reactions are associative in mechanism. Complexes that undergo dissociative substitution are often co-ordinatively saturated and have octahedral molecular geometry. The entropy of activation is characteristically positive for these reactions, which indicates that the molecularity of the reacting system increases on going from the initial to the transition state (TS). Analogous to S_N1 mechanisms, these dissociative pathways are characterized by a rate determining step that involves release of a ligand from the coordination sphere of the metal undergoing substitution. Consequently, the concentration of the substituting nucleophile has no influence on the rate and an intermediate of reduced coordination number can sometimes be detected. Although the 18-electron rule would suggest non-reactivity in either a stoichiometric or catalytic sense, there are many exceptions. Complexes with fewer than 18 valence electrons tend to show enhanced reactivity.

The composition of enantiomerically enriched products is traditionally expressed as the percent enantiomeric excess ee, defined as:

$$\%\ \text{ee} = ((R - S) \times 100/(R + S))$$

where R and S are the respective fractions or percentages of enantiomers in a mixture. With a given % ee the fraction of the main isomer, say R, is given by:

$$\%R = 50 + \text{ee}/2$$

The use of ee has been criticised and a preferred term is enantiomer ratio which can be expressed as a number, q (*i.e.* as a ratio having a denominator of 1), or as a ratio normalized as a percent (*e.g.*, er = 90 : 10).[1] Enantioselective synthesis is usually achieved under conditions of kinetic control so that a prochiral substrate, S, yielding enantiomeric products, P_R and P_S, is determined by the relative rates of formation of the two products, with rate constants k_R and k_S, respectively (eqn 1).

School of Chemistry, University of Edinburgh, Joseph Black Building, David Brewster Road, Edinburgh EH9 3FJ, UK. E-mail: mike.page@ed.ac.uk

This journal is © The Royal Society of Chemistry 2020

Open Access Article. Published on 11 December 2019. Downloaded on 2/7/2026 6:23:02 AM.
This article is licensed under a Creative Commons Attribution-NonCommercial 3.0 Unported Licence.

The product ratio (P_R/P_S) is given by (eqn (2)) where $\Delta\Delta G^{\ddagger}$ is the difference in free energies of activation for the formation of P_R and P_S whereas the relationship between %*ee* and k_R/k_S is given in eqn (3).

$$P_R \underset{k_R}{\overset{\text{cat}}{\leftarrow}} S \underset{k_S}{\overset{\text{cat}}{\rightarrow}} P_S \quad (1)$$

$$\frac{P_R}{P_S} = \frac{k_R}{k_S} = e^{-\Delta\Delta G^{\ddagger}/RT} \quad (2)$$

$$\frac{k_R}{k_S} = \frac{100 + ee}{100 - ee} \quad (3)$$

If the synthesis involves, say, nucleophilic addition to the prochiral faces of an electrophile in the presence of a chiral catalyst the free energies of activation for the addition to the *Si* and *Re* prochiral faces are not equal. The larger the difference in the free energy difference between the pro-*R* and pro-*S* transition states ($\Delta\Delta G^{\ddagger}$), the greater is the enantioselectivity. For example, a $\Delta\Delta G^{\ddagger}$ = 5.7 kJ mol^{-1} at 298 K gives an enantiomer ratio of 10 : 1 and an ee of 82% (Table 1).

The changes in concentration of the reactant substrate [*A*] and enantiomeric products [*R*] and [*S*] (eqn (1)) with time are given by eqn (4)–(6).

$$[A] = [A_o]e^{-(k_R+k_S)t} \quad (4)$$

$$[R] = \frac{[A_o]k_R}{k_R + k_S}\left(1 - e^{-(k_R+k_S)t}\right) \quad (5)$$

$$[S] = \frac{[A_o]k_S}{k_R + k_S}\left(1 - e^{-(k_R+k_S)t}\right) \quad (6)$$

An assumption in the above treatment is that P_R and P_S are not in equilibrium and are formed with the same kinetic order *e.g.* say both are first or second order. It is later described that this is not always the case which may mean that the enantiomer ratio is dependent on the concentration of substrate.

In general, an activated Ir catalyst (Ir_{cat}) can react with a substrate S through initial complex formation to give intermediate species after chemical reaction and eventually to generate bound product before product release and catalyst regeneration (Scheme 1).

Table 1 The ratio of rate constants k_R/k_S for enantiomer formation and corresponding %ee and differences in free energies of activation for eqn (1)

k_R/k_S	%*ee*	$\Delta\Delta G^{\ddagger}$ (kJ mol^{-1})
2	33.3	1.7
5	66.6	4.0
10	81.8	5.7
25	92.3	8.0
50	96.1	9.7
100	98.0	11.4
1000	99.8	17.1

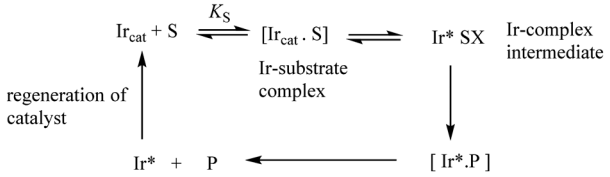

Scheme 1 Possible pathway for the iridium catalysed reactions.

The binding of S and intermediates can be very weak or so strong that they accumulate and represent the major Ir species present under the reaction conditions. Consequently, the rate of reaction can show saturation kinetics *i.e.* zero-order in substrate. A rate independent of substrate concentration can be indicative of a rate-limiting step involving the catalyst bound to substrate, intermediate or product or regeneration of the catalytic species. If coordination is strong and an apparent binding constant can be measured it is important to remember that this constant is the overall binding constant of all Ir-bound species and not necessarily K_S (Scheme 1), *e.g.* the Ir*SX intermediate may accumulate and represent the major Ir species present under steady-state conditions.

2. External factors affecting enantioselectivity

Later sections will emphasise the importance of the catalytic iridium structure, particularly the ligands and oxidation state of the metal-ion, and the nature of the substrate that influence reactivity and selectivity, but here other external factors are briefly discussed.

In general, for a catalysed conversion of an achiral substrate into a chiral product, any enantioselectivity results from the differences in the free energies of the transition states of the two enantiomers being formed (eqn (2)). Changing the solvent does not change this conclusion, although relative reactivities in the rates of formation of the products in the two solvents can sometimes result from changes in the free energies of the achiral reactants and catalyst in the two solvents as well as transition state effects.[2] For example, good reactivities and selectivities in the Ir(I) catalysed reduction of imines with hydrogen are often favoured in dichloromethane and toluene.[3] Solvents may interact directly with the catalyst, substrate and product which can therefore increase or decrease reactivity and selectivity.[4] There are many solvent properties which can influence these parameters and include polarity, hydrogen-bond donating and accepting ability, basicity and nucleophilicity.[5] Interaction or coordination of the solvent with the catalyst can influence catalytic stability, activity and selectivity. The degree of ion-pairing between a charged catalyst and counter-ion charged substrate can be greatly affected by the nature of the solvent and hence catalytic activity. Similarly, a solvent poor at solvating ions can have an impact on ion-pairing between a positively charged

Open Access Article. Published on 11 December 2019. Downloaded on 2/7/2026 6:23:02 AM.
This article is licensed under a Creative Commons Attribution-NonCommercial 3.0 Unported Licence.

catalyst and its counter-anion and so influence catalytic activity. This can be adverse if the counter-ion blocks the active site of the catalyst by blocking the vacant coordination site where the substrate may bind.[6] If there is an increase in polarisation – charge density – of the transition state compared with the reactant state, including the catalyst, then using a more polar solvent will increase the rate of reaction. Conversely, a less polar solvent will stabilise the transition state if its polarisation is less than that of the reactants, thus increasing the rate of reaction.[7] A solvent that preferentially stabilizes one of the enantiomeric transition states controlling selectivity should enhance the enantioselectivity of the product *i.e.* changes the ratio k_R/k_S.

Several reactions using iridium catalysts involve reduction with gaseous hydrogen and the mass transfer of gases can sometimes be affected by the solvent viscosity leading to a reduction in the rate of reaction or even changes in selectivity. For example, the rate of hydrogenation of imines by a cyclometallated iridium complex containing an imino ligand increases linearly with hydrogen pressure but is zero-order in imine concentration compatible with Ir-hydride formation rather than hydride transfer to the imine.[8] Highly viscous solvents generally have low rates of mass transfer of gases which can affect both rate and selectivity.[9]

Changing the temperature generally has only a small effect on enantioselectivity.[10,11] A difference in activation energies for formation of two enantiomeric products of 12 kJ mol^{-1} requires a temperature change of 50 °C to give a difference in their rates of formation, k_R/k_S, of 2.

The role of various additives has been explored including changing the anion associated with positively charged catalysts. Other common additives include bases, acids and metal-ions. Many iridium catalyzed reactions involve nucleophilic attack on an unsaturated centre and the addition of electrophiles such as a proton or metal-ion may facilitate this by coordination to the unsaturated substrate (Scheme 2). The proton is more effective than even multiply charged metal-ions. The reactivity and selectivity of the hydrogenation of the imine *N*-(1-phenylethylidene)-benzylamine using the chiral Ir catalyst, [Cp*IrCl{(*S*,*S*)-Tscydn}], is increased by the presence of silver salts. An excess of $AgSbF_6$ increased enantioselectivity by up to 72% ee which is attributed to coordination of Ag^+ to the imine nitrogen facilitating hydride transfer from Ir–H.[12]

3. Historical background

Homogeneous iridium catalysis had a slow start mainly because it apparently displayed no special properties compared with other platinum metals. Vaska[13] prepared several iridium species (Scheme 3) in which co-ordinatively unsaturated Ir(I) **1a** reacted with a variety of A–B molecules to give the corresponding oxidative addition octahedral Ir(III) products **1b**. This formally represents a two electron transfer from Ir to A–B and a change in oxidation state of the metal-ion and so is referred to as oxidative addition. The importance of these new complexes centres on the addition of small ligands and serves as the platform for homogeneous catalysis.

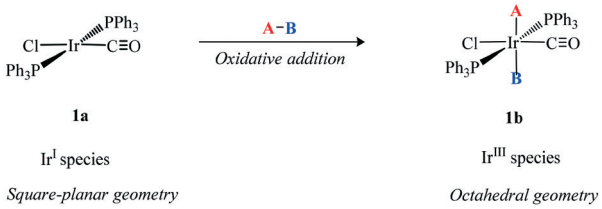

Scheme 3 Oxidative addition of A–B to Ir(I) (**1a**) species to generate the octahedral Ir(III) species (**1b**).

The ability of a transition metal compound to activate H–H bonds at ambient temperature was fundamental to later discoveries of catalysts for the homogeneous hydrogenation of unsaturated organic substrates.[14] The isolable oxidative product $Ir(III)H_2Cl(PPh_3)_3$ is extremely stable whereas relatively unstable intermediates are required for any successful catalytic protocol. The dissociation of a ligand to generate a vacant coordination site for the substrate or reactant to bind is often a pre-requisite for a catalytic cycle. The main reason for the lack of dissociation of the phosphine ligand in the iridium complex compared with rhodium is due to the increase in bond strength on going from the second to third row of the transition metals. This factor has been one of the disadvantages of using iridium in catalytic processes.

Due to the isoelectronic nature of iridium and rhodium advances in either area have often been transferred and tested on the respective counterpart. The discovery by Schrock and Osborn that **2** could be converted *in situ* to **3** demonstrated that dissociation of the ligand was not restricted to phosphine ligands.[15] This discovery not only paved the way for Crabtree's catalyst **4** but also offered the possibility of incorporating other chelating ligands including chiral ones (Scheme 4).[16]

After the discovery that coordinating solvents such as acetone, ethanol and THF resulted in complexes $[M(cod)L_2]ClO_4$ (cod = 1,5 cyclooctadiene) which reacted with hydrogen to obtain isolable complexes, Crabtree reported enhanced

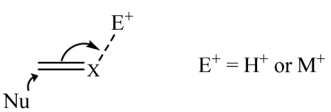

Scheme 2 Nucleophilic attack on an activated prochiral substrate.

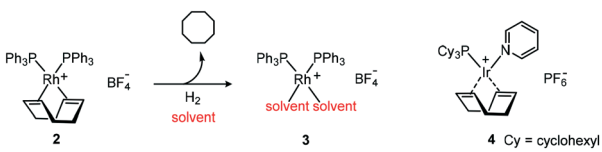

Scheme 4 COD displacement by solvent molecules.

This journal is © The Royal Society of Chemistry 2020

Open Access Article. Published on 11 December 2019. Downloaded on 2/7/2026 6:23:02 AM.
This article is licensed under a Creative Commons Attribution-NonCommercial 3.0 Unported Licence.

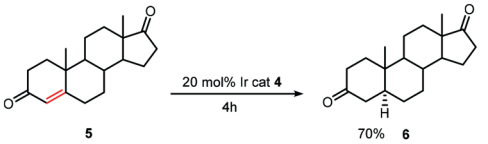

Scheme 5 Hydrogenation of steroid **5** with $[Ir(cod)L(py)]PF_6$.

catalytic activity of a series of $[M(cod)L(py)]PF_6$ (M = Rh(I), Ir(I); py = pyridine) complexes which dissolve readily in dichloromethane. The new complex **4** exhibited enhanced activity in the hydrogenation of even tri- and tetra-substituted alkenes. Whereas the coordinating solvent stabilises the iridium complexes,[17] it was demonstrated that only the alkene can stabilise the catalyst by coordination with the rhodium analogue. The higher catalytic activity indicated the critical role of the solvent in homogeneous catalysis.[18]

The hydrogenation of steroids such as **5** with $[Ir(cod)L(py)]PF_6$ **4** (Scheme 5) gave yields ranging from 70–100% and the best rates were obtained by bubbling hydrogen through the solution rather than by working under one atmosphere of hydrogen. However, steroids bearing an alcohol functionality deactivated the catalyst and so protection of this moiety was required.[19]

The coordination of the hydroxyl group can exert a stereocontrolling effect in Ir catalyzed reactions.[20] The hydrogenation of indenones with a β-OH or carbonyl gave exclusively *cis*-indanone, whereas the α-derivative in DCM gave the *trans*-indanone (*trans*/*cis* 96 : 4).

The ability of the alcohol to control the stereogenicity of hydrogenation[21] reaches an impressive 1000 : 1 ratio for the isomeric product alkanes from the reduction of terpinen-4-ol **7** (Scheme 6). The proposed intermediate complex was not observed but the more stable, but poorer catalytic, derivative $Ir(I)(PPh_3)_2^+$, binds to the hindered *endo*-5-norbornen-2-ol **10** as shown by NMR due to the sensitivity of the Ir–H chemical shift to the nature of the *trans* ligand (Scheme 7).[22]

Application of this new coordination possibility to increase selectivity was used in the synthesis of (+)-pumiliotoxin C. One of the key transformations during this synthesis (Scheme 8) was the transformation of **12**, the intermediate product **13** was obtained in quantitative yield with high selectivity.[23] A ligating group, particularly OH, in alkenes can thus bind to the catalyst and so direct addition of H_2 from that face of the molecule which contains the ligating group. Furthermore, the OH also protects the catalyst from deactivation.

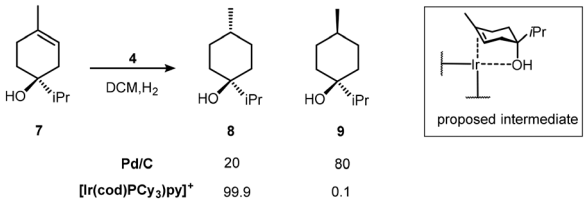

Scheme 6 Terpinen-4-ol hydrogenation with Ir catalyst **4**.

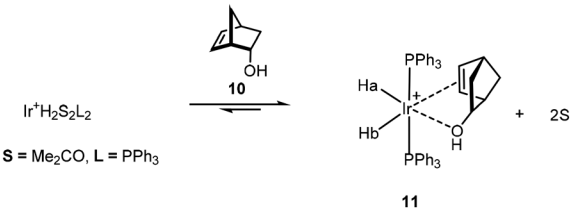

Scheme 7 Proposed structure for the stable intermediate **11**.

Scheme 8 Hydrogenation of **12**, a key intermediate in the synthesis of (+)-pumiliotoxin C.

4. Ligand development

In general iridium catalytic species can be divided into cationic(I), neutral(I) and Iridium(III) clusters, each displaying different mechanisms in their ability to transform prochiral substrates into their respective chiral counterparts.

One of the prominent examples in ligand development was the introduction of a novel BINAP (2,2′-bis(diphenylphosphino)-1,1′-binaphthyl) ligand **14** with a ruthenium complex (Scheme 9) which exhibited high reactivity and excellent selectivity for allylic and homoallylic alcohols and showed the dependency of these on the relative position of the hydroxyl group and alkene. Further developments of this catalytic protocol went on to earn Noyori the Nobel prize in 2001.[24,25]

The discovery of the chloroacetanilide (*S*)-metolachlor, one of the most important herbicides for use in maize production initiated the quest to find a viable enantioselective catalyst as 95% of the herbicidal activity of metolachlor resides in the two (1′*S*)-diastereoisomers. Although rhodium was initially recruited as the metal, the maximum ee of 69% for this process was not viable on an industrial scale and so attention turned to using iridium with a BDPP ligand giving 84% ee. A disadvantage was that the catalyst suffered from active complex dimerization **19**, an irreversible process (Scheme 10).[26]

The enantioselective hydrogenation of 2-methyl-1,2,3,4-tetrahydroquinoxaline (MeQ) using the *ortho*-metallated dihydride complex *fac-exo*-(*R*) **22** as the catalyst precursor increased ee using methanol as the solvent rather than usual DCM.[27] The two imines are hydrogenated at similar rates.

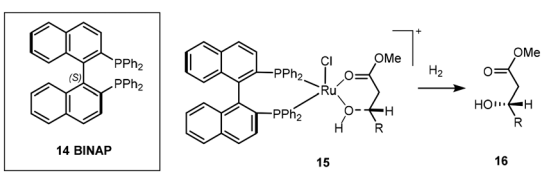

Scheme 9 Stereo-directing binding effect of BINAP for Ru dihydride reduction to afford chiral product **16**.

Open Access Article. Published on 11 December 2019. Downloaded on 2/7/2026 6:23:02 AM.
This article is licensed under a Creative Commons Attribution-NonCommercial 3.0 Unported Licence.

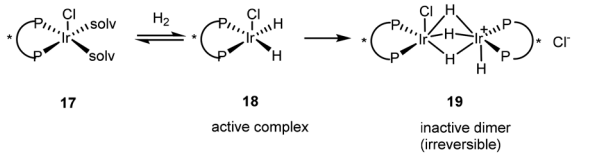

Scheme 10 Catalyst deactivation *via* active complex **18** dimerisation.

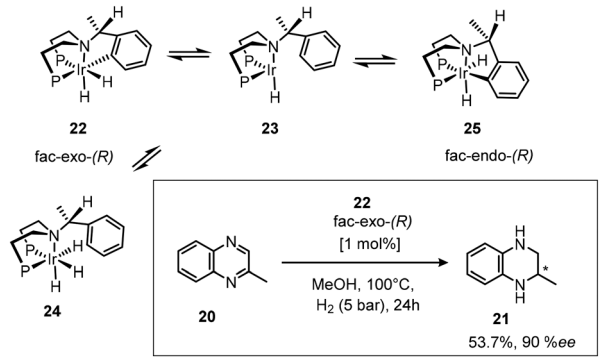

Scheme 11 *ortho*-Metallated dihydride complex catalytic species.

The sixteen electron intermediate **23** (Scheme 11), is thought to be the active catalytic species, coordinating the substrate imine, allowing hydride transfer to give an anionic amine species, followed by hydrogen oxidative addition and reductive elimination of the product amine to complete the cycle with regeneration of the catalyst.

The introduction of a chiral phosphane ligand, (*R*,*R*)-f-binaphane **39**, modified by a ferrocene backbone, altered the electronic and steric properties of the resultant catalyst (Scheme 12).[28] The low rotation barrier of the ferrocene backbone offers flexibility which can facilitate binding of sterically demanding imines to the Ir centre, and more importantly the strong electron back-donating ability from an Ir complex to an imine substrate is increased by the electron-donating f-binaphane ligand with a large P–Ir–P bite angle. A significant change in the enantioselectivities was observed in the presence of I_2.

4.1 Ligands for neutral iridium(I) catalysts

The following section will provide a brief coverage of neutral Ir(I) complexes as one of the key catalytic species in transfer hydrogenation of various substrates. Bis(1,5-cyclooctadiene) (COD) diiridium(I) dichloride **30** serves as the main precursor and the ancillary labile COD ligands allow for complex

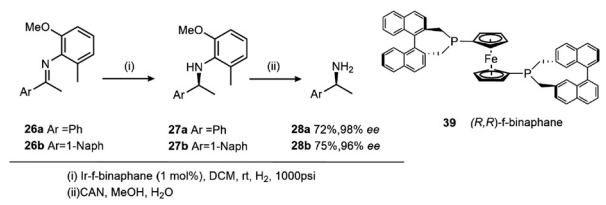

Scheme 12 Asymmetric hydrogenation of **26** using **39**.

architecture to be introduced around the metal centre by various ligands (Scheme 13, **31**–**48**); providing rich chiral environments for hydrogenation processes.

The introduction of chiral phosphine ligands had a tremendous impact on iridium catalysed reactions of industrial interest. A series of diphosphinoiridium complexes[26] for the enantioselective hydrogenation of *N*-aryl ketimines were synthesised and among this crop of ligands BDPP (2*S*,4*S*)-2,4-bis(diphenylphosphino)pentane **31** (Scheme 13) gave rise to highly reactive complexes capable of good activity and enantioselectivities due to the conformationally flexible six- or seven-membered metallacycle (Scheme 14).

The asymmetric hydrogenation of ketimines by a neutral Ir(I) complex of (4*R*,5*R*)-MOD-DIOP((4*R*,5*R*)-2,2-dimethyl-1,3-dioxolane-4,5-diyl) bis(methylene)bis(bis(3,5-dimethylphenyl)-phosphine) **32**, a derivative of the original DIOP ligand produced an efficient reduction of 2,3,3-trimethylindolenine **51** (Scheme 15). The introduction of *p*-methoxy and *m*′*m*-dimethyl groups into the phenyl groups of biphosphine ligands improved the enantioselectivity of this Ir(I) complex to 81.4% ee.[29]

The development of Josiphos, extremely modular and tunable chiral ferrocenyl diphosphine ligands, provided very efficient ligands for several commercial applications.[30,31] Xyliphos **53**, (Scheme 16) was capable of full conversion of the substrate **49** in 4 h with 79% ee. This hydrogenation not only represents the largest enantioselective catalytic process in use in industry, but also presented one of the fastest homogeneous systems known, second only to certain Ziegler–Natta polymerization catalysts.[32]

Some heteroaromatic compounds with resonance stability that retards reduction and also contain nitrogen and sulfur atoms capable of poisoning catalytic species are a challenge to asymmetric transfer hydrogenation (ATH). Employing choloroformate as an activating agent partially disrupts aromaticity by the formation of quinolinium and isoquinolinium salts so that the ATH of quinolines and isoquinolines could be achieved with 83 and 90% ee's respectively.[33] Ir(I) complexes with BCPM and MCCPM **42** (Scheme 13) in the presence of tetrabutylammonium iodide or bismuth(III) iodide were applied in the reduction of 2,3,3-trimethylindolenine and other cyclic imines with impressive enantioselectivities up to 91% ee and conversions of around 92%.[34] New phosphine–phosphoramidite ligands containing two elements of chirality were among a new crop of ligands introduced, **43** proved to be very efficient for the ATH of 2-substituted quinolones with 99% yields and 97% ee.

In an effort to improve access to sterically hindered chiral amines a family of unsymmetrical hybrid phosphine phosphoramidite ligands **41** where developed.[35] Modification of the binaphthyl backbone to further improve the overall catalytic performance by increasing steric hindrance on the amino moiety and chiral carbon centre of this ligand resulted in high turnover numbers (up to 100 000) and good enantioselectivities (up to 99% ee) for the hydrogenation of a variety of sterically hindered *N*-arylimines. These results

 This journal is © The Royal Society of Chemistry 2020

Open Access Article. Published on 11 December 2019. Downloaded on 2/7/2026 6:23:02 AM.
This article is licensed under a Creative Commons Attribution-NonCommercial 3.0 Unported Licence.

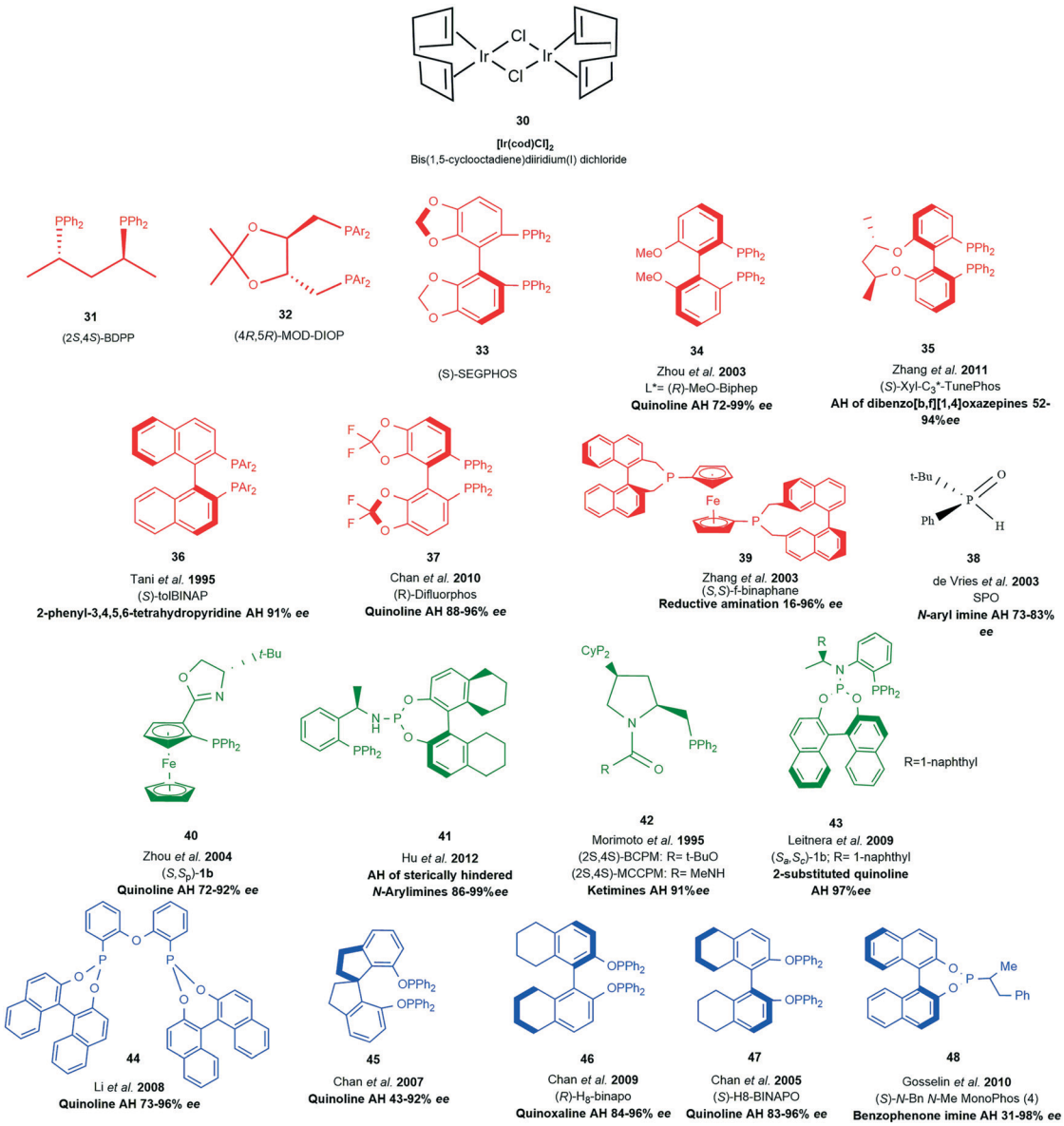

Scheme 13 Ligand examples with $[Ir(cod)Cl_2]_2$ serving as the precursor. **RED** (diphosphino ligands), **BLACK** (phosphino oxide) **GREEN** (phosphine phosphoramidite P–N ligands), **BLUE** (diphosphonite ligands).

indicated that the presence of an N–H proton on the amino moiety and a H_8-binaphthyl moiety on this ligand is crucial for achieving high catalytic activity and enantioselectivity. The utility of this catalytic system was demonstrated by the synthesis of the chiral herbicide (1*S*)-metolachlor at a catalyst loading of 0.001 mol%.

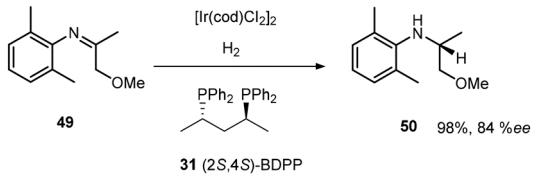

Scheme 14 Chiral diphosphine ligand utility in the synthesis of **50**.

(*R*)-MeO-Biphep **34** represented the first example of a highly enantioselective iridium/phosphine/I_2 catalytic system for the hydrogenation of quinolines; an efficient methodology granting access to a variety of optically active

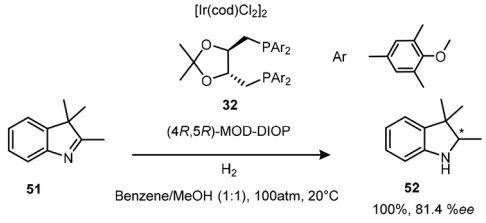

Scheme 15 Hydrogenation of 2,3,3-trimethylindolenine with the newly developed ligand **32**.

Open Access Article. Published on 11 December 2019. Downloaded on 2/7/2026 6:23:02 AM.
This article is licensed under a Creative Commons Attribution-NonCommercial 3.0 Unported Licence.

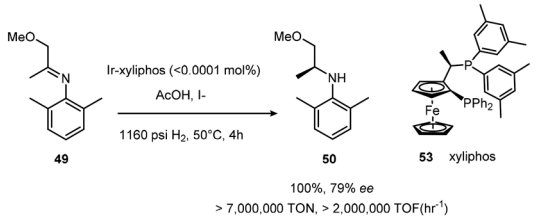

Scheme 16 Hydrogenation of **49** with **53** resulting in enhanced conversion capability.

tetrahydroquinolines with up to 96% ee. This methodology was successfully applied to asymmetric synthesis of tetrahydroquinoline alkaloids providing examples of access to naturally occurring tetrahydroquinoline alkaloids angustureine, galipinine and cuspareine in high yields.[36]

Following the highly enantioselective catalytic asymmetric hydrogenation of quinolines with MeO-Biphep/I_2 as the catalyst system, ferrocene derived phosphino-oxazoline ligands **40** gave up to 92% ee's. The chiral *N,P* ligands of ferrocenyl–oxazolines derived from different amino alcohols show varied effectiveness for the enantioselectivity with absolute configuration of the product being mainly controlled by the central chirality of the oxazoline ring.[37]

A highly modular and inexpensive chiral phosphoramidite ligand **48** provided a protection-free approach to asymmetric synthesis of diarylmethylamines.[38] This environmentally sound, and atom-economical approach performing well under acidic reaction conditions yielded 18 examples with ee ranging from 31–98%. The necessity for *ortho* substitution of benzophenone N–H imines was noted as being a key feature for obtaining high enantioselectivity. It was also reported that the enantioselective hydrogenation of seven-membered substituted dibenzo[*b*,*f*][1,4]oxazepines provided an efficient route to optically active 11-substituted-10,11-dihydrodibenzo-[*b*,*f*][1,4]oxazepines. The sterically hindered (*S*)-Xyl-C_3*-TunePhos **35** gave the highest enantioselectivity, providing 13 examples with ee's ranging from 52–94%.[39]

An Ir(I)-(*S*)-tolBINAP-protic amine catalytic system **36** for the asymmetric hydrogenation of the cyclic imine, 2-phenyl-3,4,5,6-tetrahydropyridine achieved an enantioselectivity of 90%. Enhanced catalytic activity was observed with the addition of sub-stoichiometric addition of MeOH or EtOH without impairing the enantioselectivity.[40]

Chiral diphosphonate ligands, derived from BINOL with an achiral diphenyl ether backbone, are excellent for the Ir-catalyzed asymmetric hydrogenation of quinolines. The ligand **44** comprises a diphosphonite derived from BINOL and an achiral backbone originating from diphenyl ether.

An Ir-f-binaphane complex **39** allows for the complete conversions and high enantioselectivities (up to 96% ee) in the asymmetric reductive amination of aryl ketones in the presence of $Ti(OiPr)_4$ and I_2. Formation of the imine substrate appears to be the limiting step, however the approach to avoid isolation and purification of this substrate allows for the asymmetric reductive amination of ketones or aldehydes with amines to be undertaken in a simple and practical method for the preparation of chiral amines.[41]

By employing an easily accessible H8-BINAPO chiral phosphinite ligand **47** for the ATH of quinolines derivatives it was demonstrated that the ligand provided better enantioselectivities in the less polar biphasic system poly (ethylene glycol) dimethyl ether (DMPEG, MW1/4500)/hexane reaction medium than in THF; with up to 11% increase of enantioselectivity being observed compared with those obtained in THF.[42] An iridium catalyst containing a new chiral phosphinite ligand Spiropo **45** derived from (*R*)-1,19-spirobiindane-7,79-diol exhibits high catalytic activity (substrate/catalyst ratio up to 5000 with 91% conversion) and excellent enantioselectivity (up to 94% ee) in the asymmetric hydrogenation of quinolines. The catalytic species was noted to be stable in THF; a feat that was maintained even after two months under an inert atmosphere with activity and enantioselectivity still unchanged. If the hydrogenation was carried out in a DMPEG/hexane biphasic system this resulted in efficient separation and recycling of the catalyst. Although the conversion dropped to 40% after four runs, the enantioselectivities remained high.[43]

The use of Ir/diphosphinite **46** catalyst in the asymmetric hydrogenation of quinoxalines gives one of the highest ee values attained so far in the catalytic asymmetric hydrogenation of 2-methylquinoxaline.[44]

A high-performance catalytic system with readily available DifluorPhos **37**, a biaryl bisphosphine ligand, to enantioselectively hydrogenate a series of quinolines at high (*S*/*C*) ratios, afforded up to 96% ee with up to 43 000 TON and up to 3510 h^{-1}. The substrate scope was also extended to asymmetric hydrogenation of tri-substituted pyridines showing excellent reactivity and enantioselectivity in the hydrogenation with nearly quantitative yields and up to 98% ee.[45]

A series of secondary phosphine oxide (SPO) monodentate ligands **38** (ref. 46) have been developed and although the phosphine oxide is the most stable form at room temperature, the tautomeric phosphinite is capable of complexing with the iridium precursor. The acidic proton of SPOs was noted as having an accelerating effect upon the transition metal-catalysed hydrogenation of imines. Higher rates were obtained with SPO/Ir ratios of 1, but this decreased enantioselectivity. An increment to a ratio of 2 (SPO/Ir) resulted in increased enantioselectivity. Additives such as *n*-Bu_4NI, K_2CO_3, *t*-BuOK, Na_2CO_3, primary amines, phthalimide, CF_3CO_2Ag and $AgBF_4$ were found to have a negative effect on hydrogenation.

4.2 Ligands for cationic iridium(I) catalysts

Of significance in the development of cationic Ir(I) complexes was the introduction of diphosphine ligands including the synthesis of phosphinooxazoline (PHOX) derivatives.[47] The phosphanodihydrooxazole had been used in Pd-catalysed allylic substitution,[48] allylic amination[49,50] and the Heck reaction.[51] The new catalyst paved the way for one of the

 This journal is © The Royal Society of Chemistry 2020

Open Access Article. Published on 11 December 2019. Downloaded on 2/7/2026 6:23:02 AM.
This article is licensed under a Creative Commons Attribution-NonCommercial 3.0 Unported Licence.

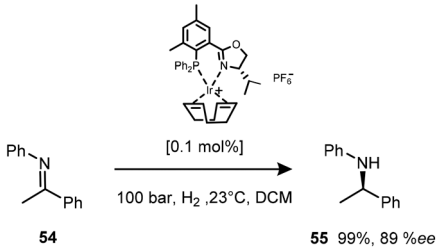

Scheme 17 ATH of the imine **54**.

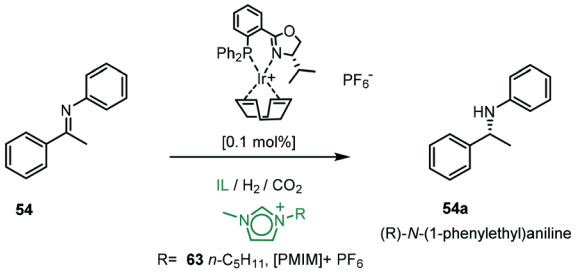

Scheme 19 Hydrogenation of **54** in various ionic liquids (IL).

most important transformations in organic chemistry – the asymmetric transfer hydrogenation of imines to afford amines (Scheme 17). This air stable complex is able to convert imines to amines with an ee of 89%.[52]

Only the catalytic asymmetric hydrogenation of unfunctionalised tri-substituted alkenes had been reported using the chiral C_2-symmetric titanocene catalyst which gave yields ranging from 70–94% with ee's of 83–99%.[53] However, the high catalyst loading required for this protocol (>5 mol%) limits its applications and so the introduction of novel chiral ligands further enhanced the potential of iridium complexes as catalysts.[54]

The functionalisation of 2-azanorbornane-oxazoline with phosphine led to novel PHOX ligands.[55] A decrease in reaction rate and enantioselectivity was observed for substrates bearing an *o*-methyl substituent. Imines with electron withdrawing groups were reduced with high yields and %ee (Scheme 18). The analogous **62** however did not display any activity in the reduction of imines but it did show high activity in the hydrogenation of acyclic and cyclic tri-substituted alkenes.

The utility of the chiral PHOX iridium catalysts was expanded using a combination of ionic liquids (ILs) and super-critical carbon dioxide ($scCO_2$). The ionic environment provides beneficial molecular interactions with the cationic organometallic intermediates (Scheme 19).[56] The CO_2 in the biphasic system allows for efficient hydrogenation in ILs, dissolving the catalyst in the IL leads to activation by anion exchange and the process allows for easy removal of the product from the catalyst solution by CO_2 extraction without cross-contamination of IL or catalyst. The highest activity was achieved in the presence of $scCO_2$ at 40 °C in 1-methyl-3-pentylimidazolium hexafluorophosphate [PMIM][PF_6] **63** with ee varying from 53–78%.[57]

Cationic Ir(I) complexes bearing aminophosphine-oxazolines (Scheme 20) were used for the hydrogenation of imines providing chiral amines up to 90% ee.[53]

Iridium complexes with phosphine–phosphite ligands demonstrate the importance of backbone flexibility on the enantioselectivity of the reaction and showing unusual better asymmetric induction with a more flexible ligand (Scheme 21).[51,58]

Examples of cationic Ir(I) and Ir(III) complexes used for asymmetric hydrogenation are shown in Scheme 22. Using an *in situ* prepared iridium catalyst based on the cheap chiral monodentate ligand (*S*)-PipPhos **68** a new low pressure hydrogenation method of a range of acyclic *N*-aryl imines was developed with excellent enantioselectivities.[59]

Unfunctionalised enamines present challenging substrates in asymmetric hydrogenation but cationic Ir(I) complexes with chiral oxazoline or pyridine-based *N,P* ligands are active catalysts for their reduction (Scheme 23). Complexes **69** and **70** exhibited excellent activity giving full conversion with low catalyst loading (0.5–1 mol%). High ee's were attributed to substitution at the C=C and the nitrogen atom with *N*-aryl or *N*-benzyl groups providing beneficial effects on the enantioselectivity.[60]

Preparation of γ- and δ-lactams in 92–97% ee was achieved with novel class of chiral *P,N*-ferrocenyl ligands **71**; the cationic

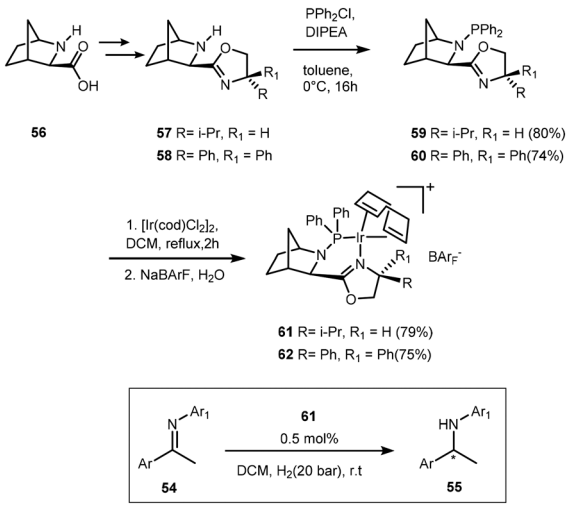

Scheme 18 Phosphine–oxazoline synthesis and utilisation in the hydrogenation of imines **54**.

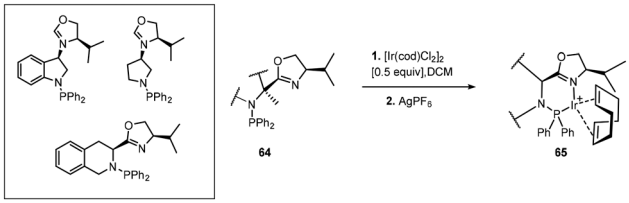

Scheme 20 Aminophosphine-oxazoline based iridium complexes.

Open Access Article. Published on 11 December 2019. Downloaded on 2/7/2026 6:23:02 AM.
This article is licensed under a Creative Commons Attribution-NonCommercial 3.0 Unported Licence.

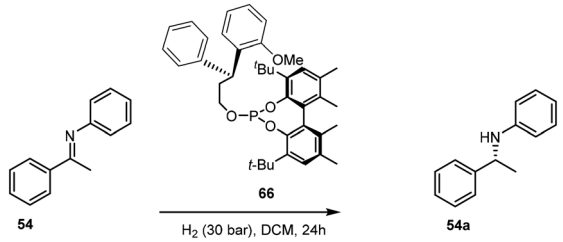

Scheme 21 Phosphine–phosphite ligands.

iridium catalyst also showing great utility in the enantioselective reduction of imines (up to 99% ee).[61] The spirobiindane scaffold is extremely rigid and bulky, a feature which was exploited in the synthesis of chiral phosphine–oxazoline ligands, providing well-defined cationic iridium complexes. A particular disadvantage of cationic iridium catalysts is that they easily form inactive trimers under a hydrogen atmosphere something that SIPHOX **72** was reported to be resistant to when exposed to a high pressure of hydrogen. SIPHOX created a crowded but efficient chiral environment around the metal centre. The catalytic system was indeed efficient in the hydrogenation of acyclic *N*-aryl ketimines, providing chiral amines in excellent ee's (>97%).[62]

Extending the chiral phosphine–oxazoline library, the iridium-catalysed hydrogenation of acyclic *N*-arylimines with **73**, induced high enantioselectivities (66–90% ee) of acyclic aromatic *N*-arylimines.[55]

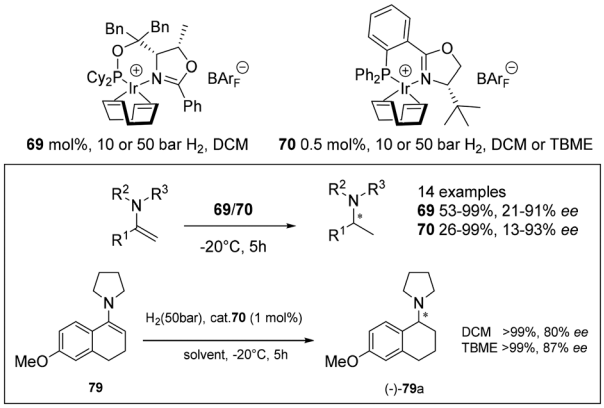

Scheme 23 Chiral oxazoline cationic Ir(I) complexes **69** and **70** for hydrogenation of enamines.

Spiro-[4,4]-1,6-nonadiene offers convenient functionalization of the backbone because the sp^2 carbon centres are well suited for further anchoring of the chelating ligation moieties during chiral-ligand construction. As well as providing excellent enantioselectivities of challenging ketimines (>98%) the cationic iridium complexes featuring chiral phosphine–oxazoline spiro-[4,4]-1,6-nonadiene backbone (SpinPHOX **74**) were subsequently employed in the asymmetric synthesis of sertraline ((+)-*cis*-(1*S*,4*S*)-1-methylamino-4-(3,4-dichlorophenyl)-tetralin, (Scheme 24) (*S*,*S*)-**81**), an antidepressant chiral drug, affording the chiral amine isomers *cis*-**81** and *trans*-**81** with

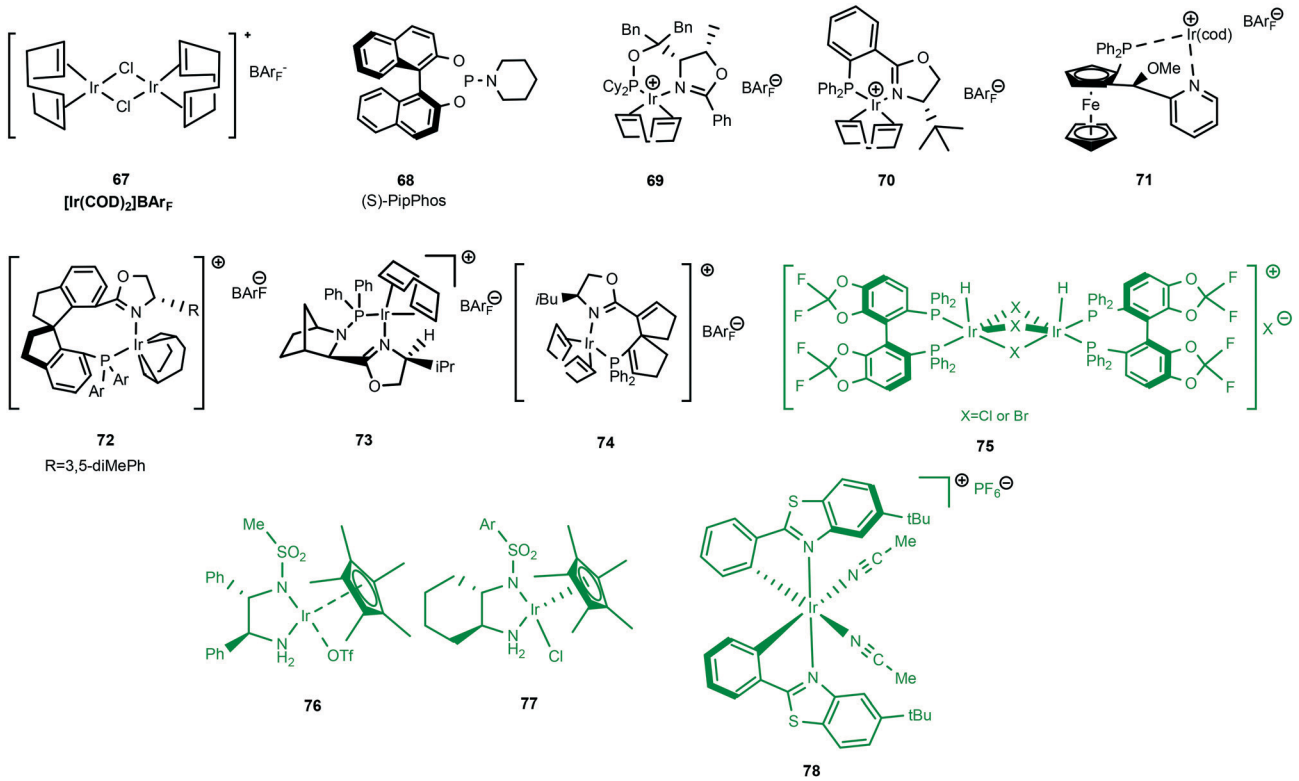

Scheme 22 Cationic Ir(I) in **BLACK** and Ir(III) complexes in **GREEN** for asymmetric hydrogenation.

 This journal is © The Royal Society of Chemistry 2020

Open Access Article. Published on 11 December 2019. Downloaded on 2/7/2026 6:23:02 AM.
This article is licensed under a Creative Commons Attribution-NonCommercial 3.0 Unported Licence.

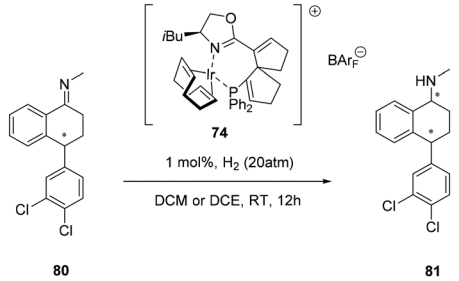

Scheme 24 Spiro-[4,4]-1,6-nonadiene phosphino-oxazoline cationic Ir(I) complex in the synthesis of sertraline **81**.

excellent enantioselectivities (89 and 98% ee, respectively) in a ratio of approximately 1 : 1.[63]

4.3 Ligands for iridium(III) catalysts

Of the three clusters encompassing iridium catalytic species, Ir(III) complexes (Scheme 22) [green] have found limited application in the reduction of imines. One of the representative examples in this class is the exceptional cationic dinuclear Ir(III) complex **75**.[64,65] The substrate scope features excellent hydrogenation of 2-aryl substituted quinolines and 2-alkyl and 2-aryl quinoxalines. Additionally, complex **75** has also proved to be formidable in the reduction of 1- or 3-substituted isoquinolinium salts.

Ir(III) complexes featuring chiral monosulfonylated diamines have indeed provided some of the highest ee's in the reduction of 2-alkyl and functionalized 2 alkyl quinolines with low catalyst loading (S/C = 500); the air stable **76** gave yields of 95% with high ee's (94–99%).[66]

Similar half-sandwich Ir(III) complexes **77** have also been reported;[12] in this work the utilisation of a cyclohexan-1,2-diamine based monosulfonylated diamine was active in the reduction of aryl methyl *N*-benzyl imines, achieving full conversion albeit with moderate enantioselectivity (39–78% ee). The efficient enantioselective ATH of ketones was achieved using bis-cyclometalated Ir(III) complex **78** with catalyst loadings as low as to 0.002 mol% (96.6% ee).[67] The rigidity of the complex limits the degree of conformational flexibility of intermediates in the catalytic cycle, an important factor that provides an entropic advantage during catalysis. The marked increase in both catalysis and enantioselectivity is also attributed to the metal–ligand cooperativity (bifunctional catalysis) due in part to the presence of the pyrazole co-ligands in the catalytic system.

5. Mechanisms of transfer hydrogenation

There are several questions to be addressed to elucidate the mechanism of iridium complex catalysed enantioselective synthesis. What is the structure of the active catalyst? Is there significant binding between the substrate and iridium complex? If so, is the binding intermolecular or does it involve significant bonding? If the latter what is the site of bonding? Are any intermediates formed? Is the reaction mechanism homo- or hetero-lytic? What is the rate-limiting step of catalysis? How is the catalyst regenerated? The previous section has catalogued an extensive library of applications of iridium catalysts in enantioselective transformations, this next section is aimed at giving a brief overview of the current understanding of mechanistic pathways encompassing this field of organometallic chemistry.

5.1 Hydrogen activation

The most common reduction catalysed by iridium complexes involves the formal hydrogen addition to unsaturated bonds generally in the form of proton and hydride transfers (Scheme 25a). The source of hydrogen can be molecular hydrogen or hydride donors such as formate anions or isopropanol (Scheme 25). Most involve iridium hydride as an active species, probably best described as a polarized covalent bond rather than as a pure ionic interaction. A particular concern in hydrogenation mechanisms is the source of the proton for reductions with molecular hydrogen in aprotic solvents and with no obvious acidic groups available. Although the formal oxidative addition of H_2 to Ir(I) to form dihydrides of Ir(III) could, in principle, provide a simple solution *via* a concerted addition to the unsaturated centre.

Generation of hydridic species from hydrogen can occur through heterolytic hydrogen cleavage [Scheme 26(a)] usually through oxidative addition, in which formally there are two electron transfers from Ir(I) to hydrogen to form two metal hydrides and a change of the oxidation state of the metal to Ir(III).[68] This of course is not an easy transformation given the H–H bond dissociation energy is 436 kJ mol^{-1}; however, transition metal complexes achieve this feat under mild conditions.

Homolytic cleavage of hydrogen [Scheme 26(b)] involves hydride transfer to Ir and proton abstraction to give a monohydride without formal change of oxidation state.[69] This process can be further split into intramolecular or intermolecular processes (mediated by an external base). Ir(III) activation by hydride donors generally yields the monohydride again with no formal change of oxidation state.[70]

Employing a sacrificial DH_2 donor [Scheme 26(c)] represents another alternative for the source of hydrogen; with the donor species transferring two hydrogen molecules to an acceptor species.

5.2 Substrate considerations

The mechanistic question about the formal hydrogen addition to unsaturated bonds in the form of proton and hydride transfers (Scheme 27) is are the steps concerted or stepwise and, if the latter, which comes first? The two prochiral substrates considered here are C=O and C=N centres. C=O substrates are well suited to undergo reduction as they are highly polarized; exhibiting weak binding to the metal. Indeed, if binding of C=O to the metal centre was

Open Access Article. Published on 11 December 2019. Downloaded on 2/7/2026 6:23:02 AM.
This article is licensed under a Creative Commons Attribution-NonCommercial 3.0 Unported Licence.

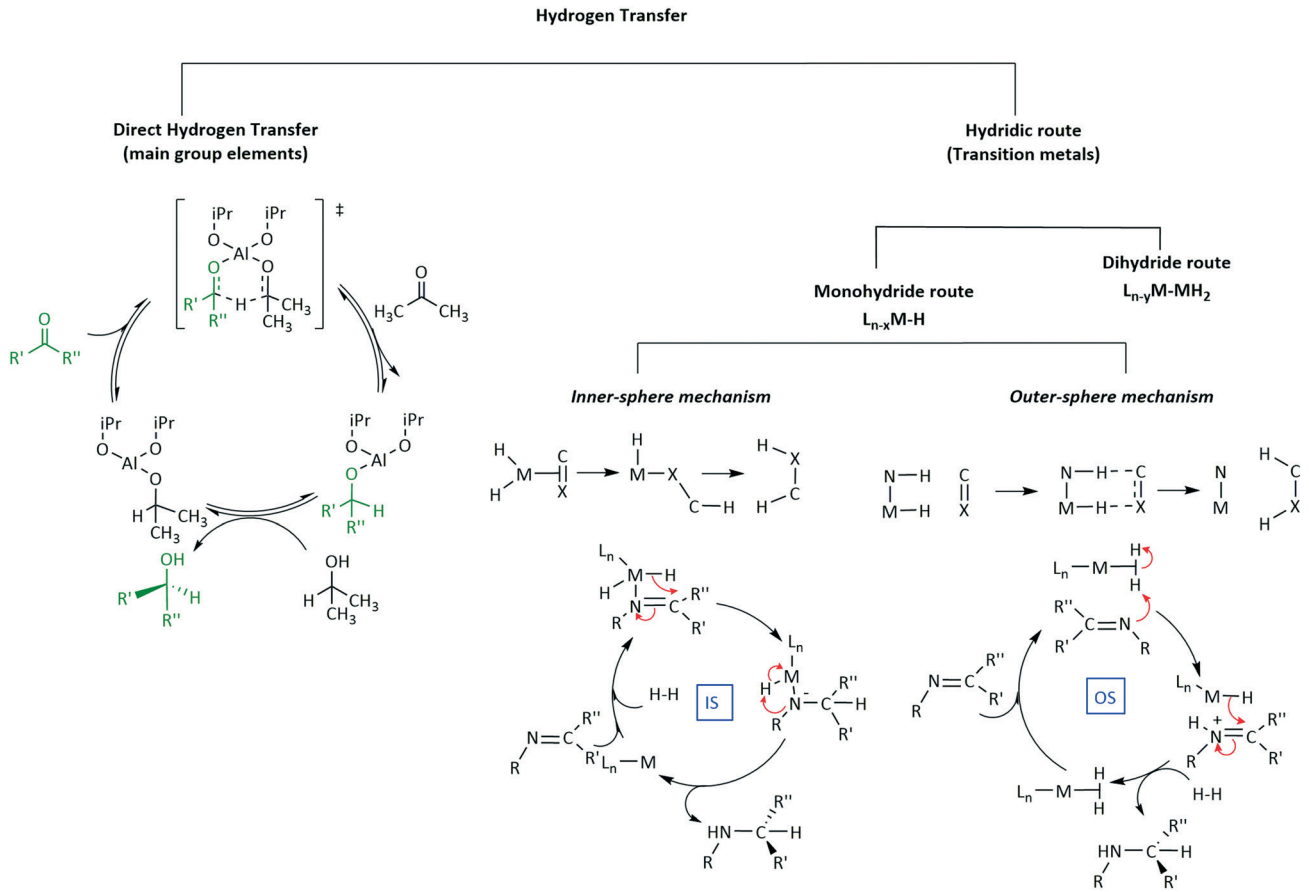

Scheme 25 Transfer hydrogenation mode using different hydrogen sources.

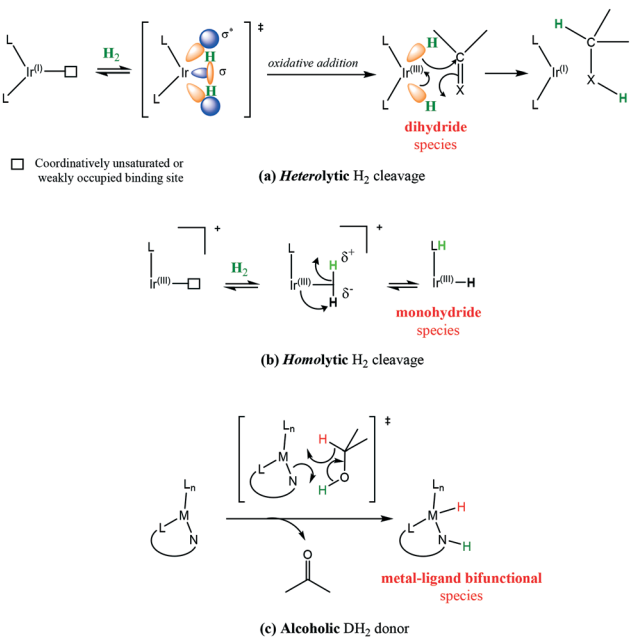

Scheme 26 Transfer hydrogenation mode using different hydrogen sources.

strong this would retard H_2 activation which is a weak ligand. On the other hand, imines are not very polarized but the lone pair residing on the nitrogen is capable of metal coordination which can suppress catalysis; prior *N*-protonation thus serves to increase its affinity for the nucleophilic addition of a hydride ion (H^-).[71]

It is sometimes suggested that proton transfer can occur from an amine NH in which this involves the formation of a very unstable nitrogen anion.[72] Similarly, hydride addition to a neutral imine generates a nitrogen anion. The pK_a of amines, involving proton loss from NH, in water is ~30 and is even higher in non-aqueous solvents such as DCM or acetonitrile and so the generation of nitrogen anions under the common conditions used in the reduction of unsaturated systems would require enormous stabilisation by other factors and seems generally unlikely.

The substrate directs classification of the reaction pathway based on the role it plays in the coordination sphere. If the

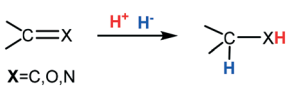

Scheme 27 Addition of H^- and H^+ across a C=X bond.

This journal is © The Royal Society of Chemistry 2020

Open Access Article. Published on 11 December 2019. Downloaded on 2/7/2026 6:23:02 AM.
This article is licensed under a Creative Commons Attribution-NonCommercial 3.0 Unported Licence.

substrate directly coordinates to the metal it is termed inner-sphere (IS) (Scheme 25b) whilst that with no coordination is outer-sphere (OS) (Scheme 25c). Those reactions involving sacrificial H donors can also be classified within these two families. Typically, in an IS mechanism (Scheme 25b), sometimes referred to as ionic hydrogenation, the substrate binds directly to the metal-ion, followed by subsequent insertion into the M–H bond, elimination of the product and oxidative H_2 addition steps to regenerate the catalyst and complete the cycle. This mechanism is common for homogenous catalysis involving iridium.[73] OS mechanisms (Scheme 25c) on the other hand do not involve direct binding of the substrate to the metal-ion but rather proceed *via* initial intermolecular interactions followed by hydride and proton transfers. The transfer of H^+ and H^- can either proceed concertedly or in a stepwise fashion to the unbound substrate. This addition of H^+ and H^- offers a sub-level classification in OS mechanisms as the processes can be considered as bifunctional or ionic mechanisms.

Bifunctional catalysis. Bifunctional catalysis (Scheme 26c) has some representative examples which feature a hydrogen with hydridic character directly bonded to the metal and another hydrogen with protic character bonded to one of the ligands in the metal complex.[74,75] In OS mechanisms the metal does not change oxidation states.[71,76]

Ionic mechanisms. Ionic mechanisms also exhibit addition of H^+ and H^- to a prochiral substrate in a step-wise fashion.[77] The insertion of the substrate into the M–H bond is not necessary as the initial step in this mechanism is proton transfer generating a neutral metallic intermediate. In the next step is a hydride transfer giving rise to the hydrogenated product. The difference in the two mechanisms is that the ionic pathway is step-wise whilst the bifunctional route is concerted.[78]

Mechanistic considerations in transfer hydrogenation have been extensively studied and while all catalysts discussed below exhibit similar features, unfortunately, some of the proposals rely more on conjecture than hard experimental evidence. This section is divided into parts, some of which involve a degree of overlap.

5.3 Outer sphere mechanisms of hydrogenation

Reduction of acyclic imines. Ionic outer sphere mechanisms have been proposed for Cp*-half sandwich iridium complexes (Scheme 28) in the direct asymmetric reductive amination (DARA) of various aliphatic ketones.[79] The mechanism follows the classic outer sphere mechanism in which imine protonation *via* Ir–$H_2(\eta^2)$ intermediate **84** is the first step with subsequent hydride transfer generating the amine product. The chiral phosphate anion was reported to enhance enantioselectivity (>99%), with suggestions of iminium-phosphate ion pair preceding the hydride transfer step.

The addition of $AgSbF_6$ in asymmetric hydrogenation of acyclic imines enhances the reactivity of the imine with diamine half-sandwich Ir(III) species, attributed to coordination of the Ag^+ to the imine nitrogen thus facilitating hydride transfer (Scheme 29). The SbF_6^- anion can be envisaged as forming an ion-pair.[11] In this outer sphere proposal, a base mediated heterolytic H_2 cleavage generates the active 18 electron monohydride species **88** which delivers a hydride to the Ag^+ coordinated imine. Protonation of the bound product results in amine formation. Whereas proton

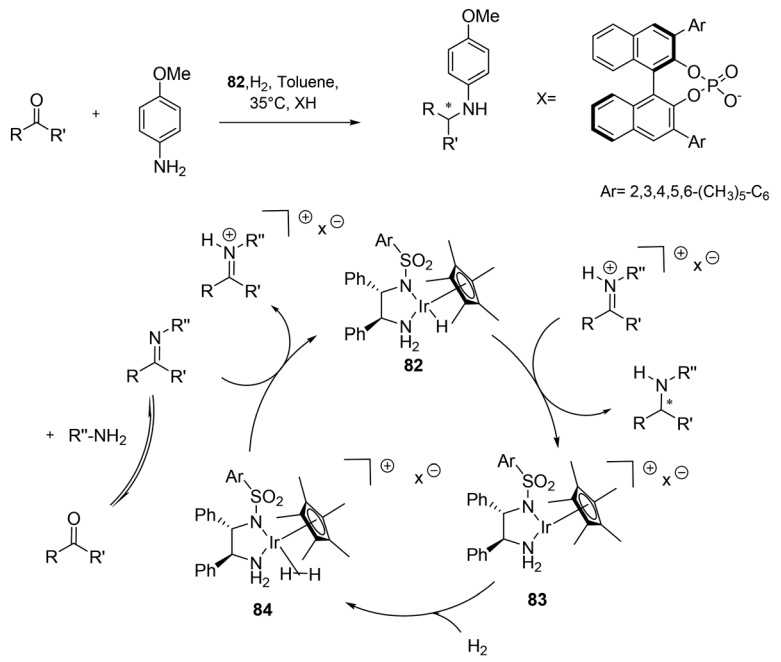

Scheme 28 Direct asymmetric reduction amination (DARA) of ketones *via* metal-counter anion cooperative catalysis.

Open Access Article. Published on 11 December 2019. Downloaded on 2/7/2026 6:23:02 AM.
This article is licensed under a Creative Commons Attribution-NonCommercial 3.0 Unported Licence.

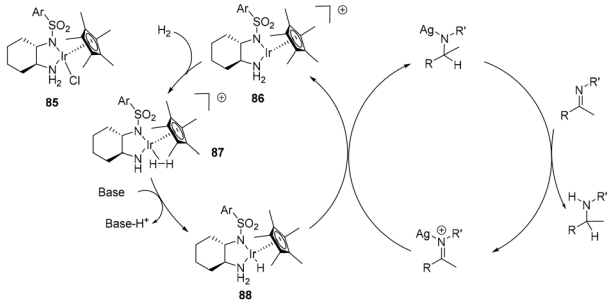

Scheme 29 Half-sandwich Ir(III) complex **85** in the Ag^+ assisted hydrogenation of acyclic imines.

transfer precedes hydride transfer in the general OS mechanism, in this proposal, Ag^+ coordination to the imine causes a reversal, thus hydride transfer occurs first, followed by protonation, although again it involves the formation of an unstable nitrogen anion.

Computational mechanistic investigations are currently leading the charge to unravel key transformations in catalytic organic processes. In a theoretical study of the PHOX system[80] an outer sphere mechanism in the asymmetric hydrogenation of acyclic imines was proposed (Scheme 30). COD hydrogenation results in the formation of a *cis*-dihydride complex **90** and an additional ligand, possibly a solvent molecule, occupies the vacant coordination site in the apical position. Though arbitrary, the solvent molecule is assumed to be stable throughout the cycle. An incoming H_2 is then assumed to coordinate in an η^2 fashion *trans* to the phosphorus ligand **91**. Formation of the active catalytic species is thus dependent on displacement of the imine by H_2. Heterolytic cleavage of the bound $H_2(\eta^2)$ by the imine results in formation of an iminium species. In an outer sphere mechanism, the iridium species **92** then delivers hydride in a stereoselective fashion to the protonated species, thus affording the amine product which is assumed to temporarily occupy a coordination site that in the next step is vacated in favour of either an imine or H_2. It is interesting to note that throughout the cycle, several inert hydride ligands are present, a justification for maintaining the +3 oxidation state.

In an unorthodox outer sphere mechanism, a ligand assisted outer sphere hydrogenation of acyclic imines (Scheme 31) **94** was proposed.[81] Fundamental to this proposal is the replacement of benzene (η^6) by an amine, exhibiting both η^6 (**94**) and η^4 (**96**) binding modes. A free amine abstracts a proton from the Ir(III) species **95** which allows for subsequent oxidative addition of dihydrogen that eventually forces the proton to migrate to the η^4 bound amine ligand, reducing the metal to Ir(I) as evidenced by H/D scrambling experiments. The rate law would agree with either a slow dissociative amine-by-imine exchange or a rate-determining bifunctional hydrogenation step. The long induction periods observed in the different solvents employed could reflect the amine-assisted dihydrogen oxidative addition step becoming the rate-determining step at low amine concentration – a feature that could be enhanced by competition of the imine for the hydrogen-bonding sites.[81] A trihydride Ir(III) complex **97** is generated by the oxidative addition of H_2 which subsequently proceeds to deliver a hydride to the carbon and a proton from the amine ligand in a bifunctional catalytic process **98**, thus affording the product amine.

Reduction of cyclic imines. Cyclic imines have less conformational freedom than their acyclic analogues which can impact the mechanistic pathway adopted.

N-Heterocyclic carbene (NHC) complexes represent a growing area of research and have been established as highly stereo-directing ligands in transfer hydrogenations.[82–87] The strong σ-donor properties exhibited by NHCs provide beneficial reactivity of the metal hydride intermediates formed during the catalysis, but also stabilize the

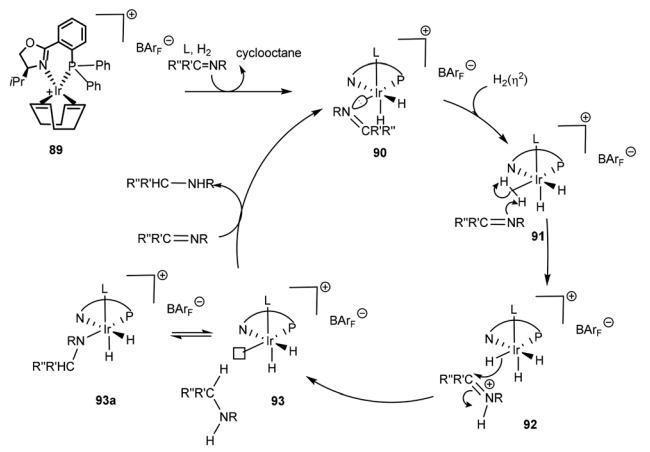

Scheme 30 Proposed inner sphere mechanism with homolytic H_2 cleavage with **89** based on a computational study.[86]

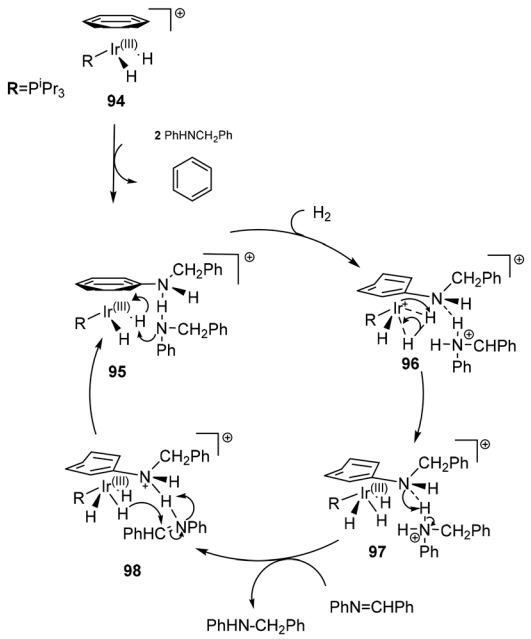

Scheme 31 Proposed outer sphere mechanism for complex **94**.

This journal is © The Royal Society of Chemistry 2020

Open Access Article. Published on 11 December 2019. Downloaded on 2/7/2026 6:23:02 AM.
This article is licensed under a Creative Commons Attribution-NonCommercial 3.0 Unported Licence.

configuration of the catalyst.[88] An outer-sphere mechanism for the **99** ATH of cyclic *N*-sulfonylimines was proposed leading to 24 examples of chiral sultams with high enantioselectivities (94–98% ee) (Scheme 32). The addition of ammonium formate is crucial in generating the catalytic species and serving as the hydrogen source. The expulsion of CO_2 and ammonia generates the active species **102**. Though not conclusive it is reasoned that generation of the 16-electron species is preceded by dissociation of MeCN or NH_3, followed by fast hydride transfer to generate a highly reactive intermediate **102**. The catalytic species then proceeds to transfer H^+ and H^- in a concerted fashion, with a hydrogen bond holding the substrate in place, subsequent product release leads to regeneration of the catalytic species. Of chief significance in the stereoselectivity is the reduced steric hindrance in the TS in addition to the hydrogen-bonding network. The outer-sphere mechanism is aided by the presence of bulky *tert*-butyl groups in the complex that restrict potential amine/imine coordination.[89]

Other outer sphere mechanisms of cyclic substrates have been proposed following a thorough investigation in the enantioselective reduction of 2-aryl-pyridinium salts with the Ir-MP (ref. 2)-SEGPHOS catalyst (Scheme 33). A series of deuteration experiments confirmed a multi-step hydrogenation cascade that involves multiple tautomerisations between the intermediate enaminium and iminium ions followed by an enantioselective addition *via* an outer-sphere mechanism. One of the challenges in hydrogenating pyridine based substrates is their strong coordination ability, a feature that can be detrimental to the catalyst. The rate of reduction of the tetra-substituted iminium was slower than that of tautomerization. Therefore, the second tautomerization had longer time to undergo a reversible process of protonation and deprotonation. A 1,4-addition was thought to be the first reduction step in the hydrogenation process with selectivity heavily relying on the geometrical fit between the catalyst and substrate. Hydride transfer and subsequent chiral reduction takes place through another outer-sphere pathway to release the final chiral piperidine to complete the catalytic cycle.[76]

The reduction of multiple bonds as in quinolines has also been proposed to occur through an outer sphere mechanism in a stepwise fashion (Scheme 34). Similar to Zhang's[76] cycle the reduction encompasses two simultaneous cycles. Initially, a 1,4-addition in the first catalytic cycle proceeds *via* step-wise proton transfer and hydride transfer to the fourth position **111**. The reduction is followed by enamine–imine isomerisation. The imine is protonated in the second cycle, leading to a final 1,2-addition, that results in the amine product.[90,94]

Reduction of ketones. The role of a strong base in hydrogenation processes has rarely been explored, but DFT calculations attempted to unravel the role played by sodium methoxide in hydrogenation processes (Scheme 35) for iridium complexes with "non-NH" ligands. A fundamental feature of this proposal was the requirement of generation of anionic species. A cycle beginning with $[Na^+(MeOH)_3]$ **113** was proposed with Na^+ anchoring the substrate. Hydride transfer to the alkoxo bound substrate then occurs; thus generating an Na^+ linked alkoxide **115** held in the Ir coordination sphere by σ C–H coordination, which then rearranges to a more stable isomer **116**. In the next step, H_2 displaces OiPr from the Ir coordination sphere **117**. The H_2 ligand then delivers a proton to the Na^+ bonded OiPr ligand to yield an iso-propanol adduct **119**, and the cycle is completed by product expulsion **113**.

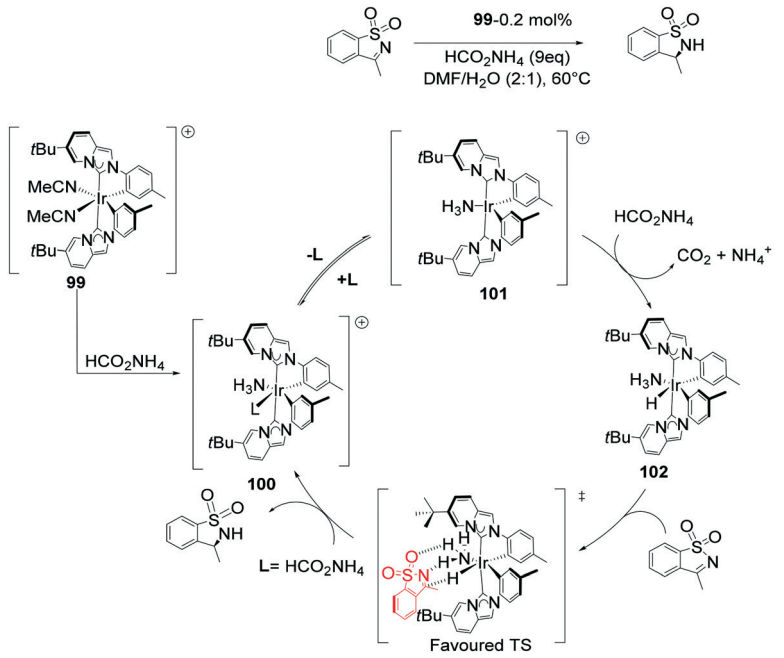

Scheme 32 ATH of *N*-sulfonylimines with a NHC furnished Ir complex **99**.

Open Access Article. Published on 11 December 2019. Downloaded on 2/7/2026 6:23:02 AM.
This article is licensed under a Creative Commons Attribution-NonCommercial 3.0 Unported Licence.

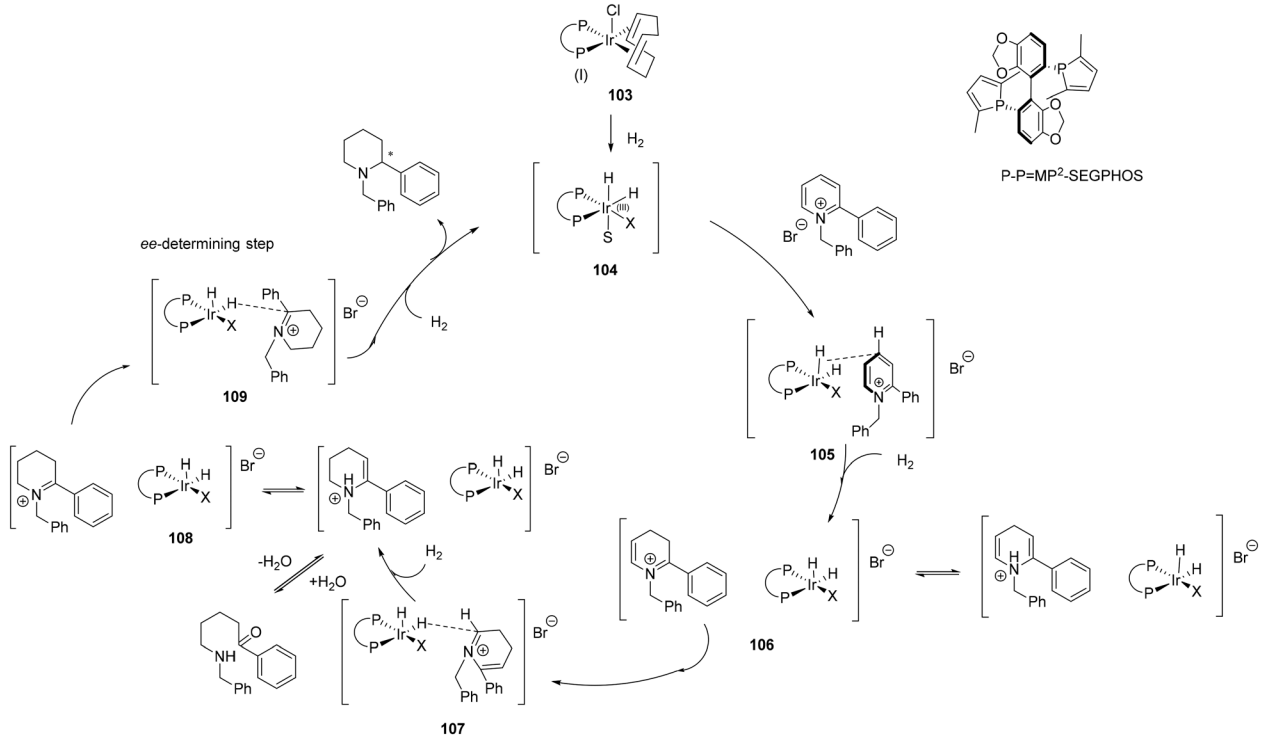

Scheme 33 Outer-sphere mechanism in the hydrogenation 2-aryl-pyridinium salts with **103**.

Therefore, the hydrogenation is in essence an outer sphere process with stepwise H^-/H^+ transfer to the sodium-activated ketone, but the proton is not initially present on the catalyst; it is only provided in a later step after H_2 activation.[91]

5.4 Inner sphere mechanisms of hydrogenation

Reduction of acyclic imines. An inner sphere mechanism for the reduction of imines involves an Ir(III) cycle (Scheme 36) in which oxidative addition of I_2 to the Ir(I) precursor **39** generates an Ir(III) complex **39a** (ref. 28) followed by heterolytic cleavage of H_2 **39b** in the presence of an amine to form the Ir(III)–H species **39c**. Migratory insertion of the η^2-imine to the Ir(III)–H gives **39d** followed by hydride transfer **39e** which forms a proposed Ir(III)–anionic amine complex **39f**

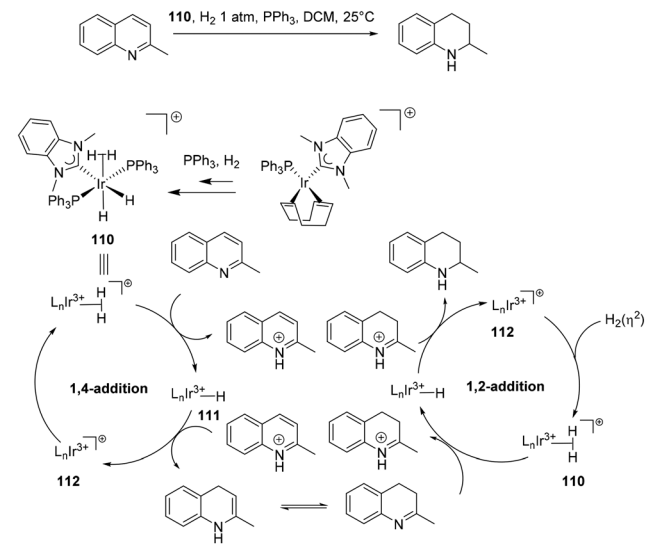

Scheme 34 The proposed mechanism for the double hydrogenation of quinolines *via* a 1,4 and 1,2-addition with **110**.

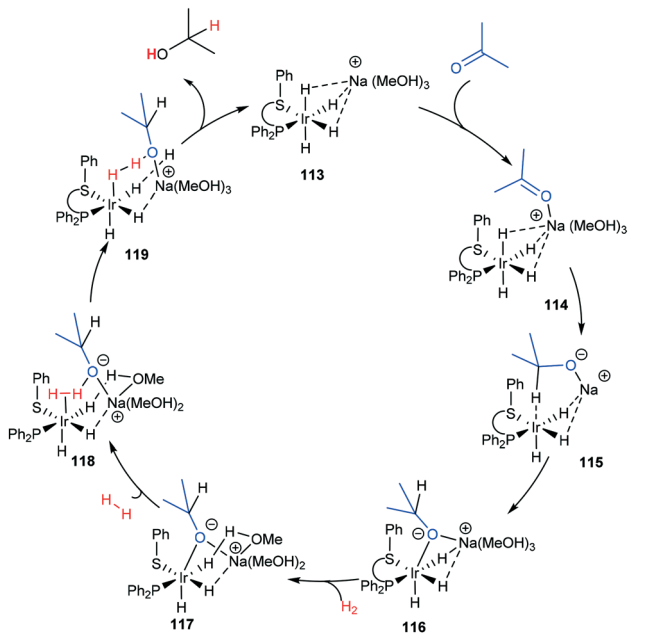

Scheme 35 Ketone outer-sphere proposal based on a DFT calculation.[97]

This journal is © The Royal Society of Chemistry 2020

Open Access Article. Published on 11 December 2019. Downloaded on 2/7/2026 6:23:02 AM.
This article is licensed under a Creative Commons Attribution-NonCommercial 3.0 Unported Licence.

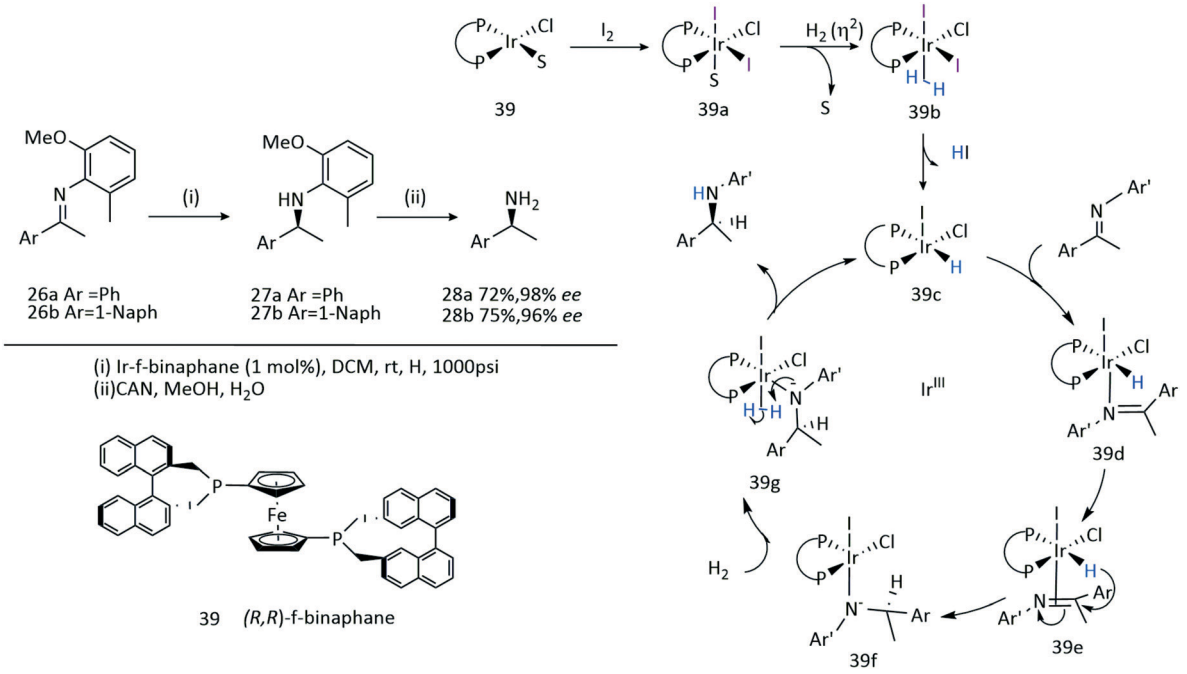

Scheme 36 Proposed catalytic cycle for hydrogenation of **26a–b** with Ir-f-binaphane **39**.

which undergoes heterolytic cleavage by H_2 **39g** to give the amine product and regenerates the Ir(III)–H species **39c**.

Reduction of Ketones. In general Ir(I) catalysts show excellent activity in transfer hydrogenation, performing better than their Ir(III) counterparts. Complexes of the class [Ir(cod)(NHC)X] that feature an ether functionality **120** proceed through the hydridic route (Scheme 37) as is common for most proposed mechanisms for Ir(III). Initial dissociation of one of the ether groups vacates a coordination site **122**; allowing for coordination of iso-propoxide which subsequently undergoes β-elimination of the C–H bond upon de-coordination. The resultant hydridic species isomerises due to the high *trans* effect of the adjacent NHC ligand, thus forcing the hydride to be *trans* to the iodide in the apical position **123**. The incoming ketone displaces the acetone product resulting in a secondary isomerisation process that releases the steric congestion in the equatorial plane **125**. This isomerisation is key for efficient migratory insertion of the ketonic substrate into the Ir–hydride bond; allowing for generation of the alkoxo complex **126**. A sacrificial ^{i}PrOH molecule then transfers a proton to the alkoxo intermediate, generating the product and thus the cycle begins again **121**.[92,93]

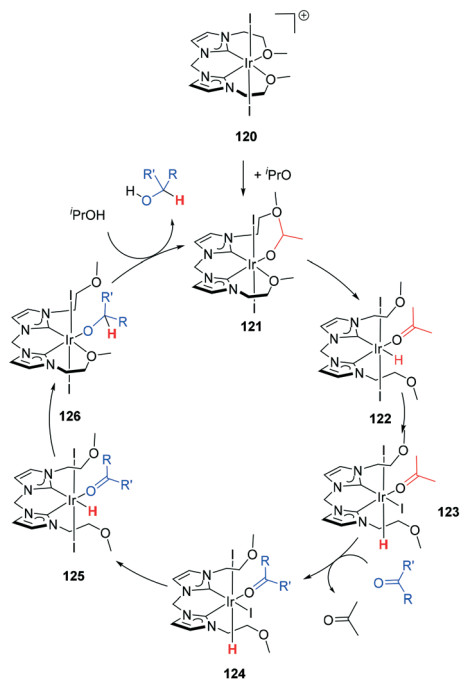

Scheme 37 Ketone hydrogenation preceding *via* an inner-sphere mechanism with **120**.

6. Hydrogen transfer steps and other mechanistic considerations

6.1 Asymmetric transfer hydrogenation

Three main pathways have been proposed (Scheme 38) for the transfer hydrogenation of ketones using iridium catalysts to give corresponding alcohol products. **Pathway A** involves a direct hydrogen transfer proceeding by means of simultaneous interaction of the substrate and hydrogen donor with the metal centre – the close proximity of these two entities results in a concerted delivery of a formal hydride from the alcohol donor to the acceptor ketone.[98,99] This pathway does not involve a metal hydride as the hydride is provided by the donor alcohol. The metal's purpose is to aid enhancement of the electrophilic nature of the carbonyl,

Open Access Article. Published on 11 December 2019. Downloaded on 2/7/2026 6:23:02 AM.
This article is licensed under a Creative Commons Attribution-NonCommercial 3.0 Unported Licence.

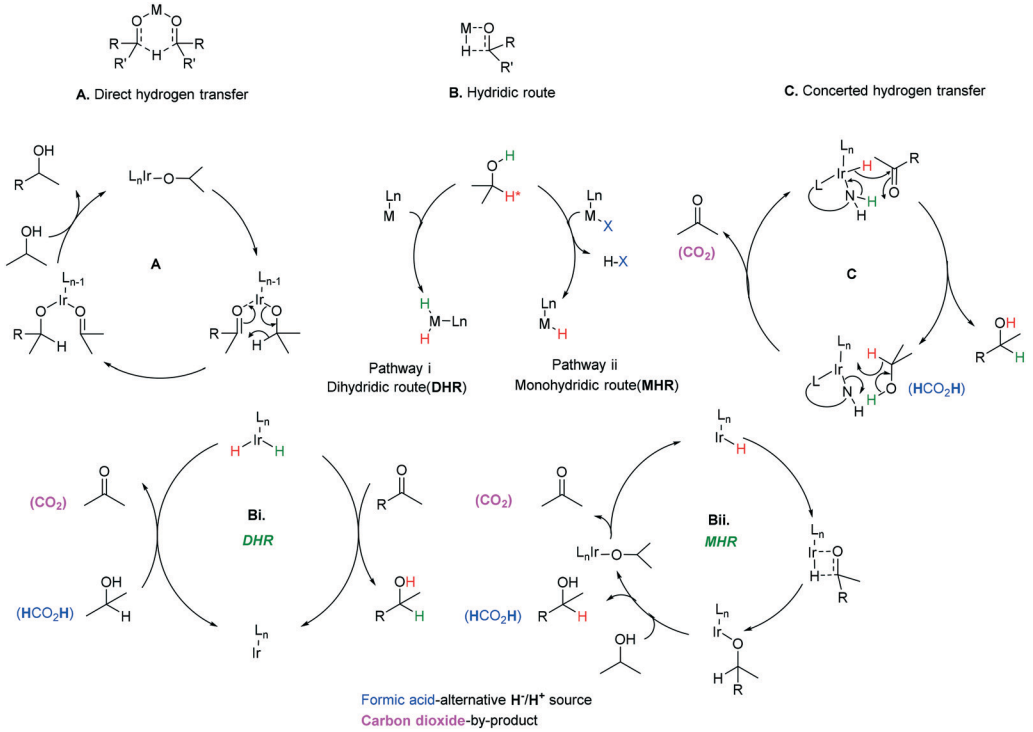

Scheme 38 Mechanisms for the ATH of ketones.

making it more receptive to the hydride attack and providing a highly organised transition state where the correct orientations for bond making and breaking are met. This direct transfer of hydrogen has been extensively studied computationally and has given support to this mechanism for some iridium catalysts.[94]

Pathway B (Scheme 38B) involves metal hydride complexes and deuterium labelling experiments have been used to probe whether hydrogen transfer proceeds through monohydride or dihydride mechanisms. The monohydride pathway (Scheme 38**Bii**) arises from the α-C–H of the donor and the dihydride results from abstraction of both the O–H and α-C–H.

In the case of Ir(I) complexes, the monohydride mechanism (**Bii**) is favoured. Activation of the H-donor occurs upon coordination of 2-propanol to the metal, providing the alkoxy complex, which subsequently undergoes an intramolecular β-hydrogen extraction to produce the metal hydride and acetone. The hydride is then delivered to the carbonyl group according to two different limiting mechanisms: (i) displacement of the coordinated acetone by acetophenone giving the alkoxide ion, followed by migratory insertion of the ketone into the metal–hydrogen bond to provide the new alkoxy derivative (inner sphere mechanism) and (ii) displacement of the alkoxy ligand from the coordination sphere of the metal by a second 2-propanol to deliver the reduced product and restarts the catalytic cycle.[95]

Delivery of hydrogen in a concerted fashion is described by **pathway (C)** (Scheme 38C) – metal–ligand bifunctional catalysis. These systems are unorthodox in that substrate reduction proceeds *via* concerted hydridic H delivery from the metal centre to the electrophilic C=O carbon, while the ligand amine NH ligand delivers a H proton to the oxygen simultaneously. The presence of an available ionisable hydrogen on the ligand is imperative and its absence results in no catalytic activity.[96,97] Catalyst regeneration then follows in a reverse process using the donor alcohol. This in turn led to the development of a repertoire of related catalysts containing an N–H functionality including iridium-based complexes (Scheme 39).[98,99]

All three reaction pathways are feasible and several factors such as the catalyst, substrate and solvent can influence which pathway is favoured by an iridium catalyst.

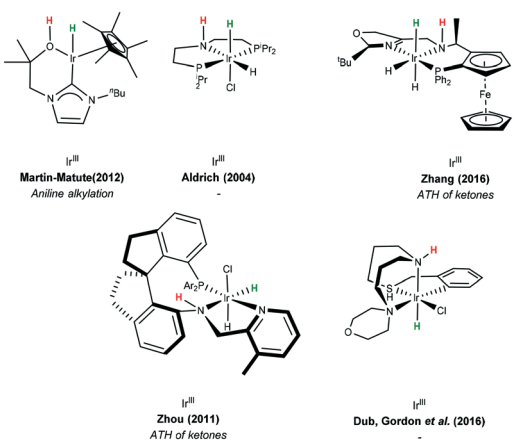

Scheme 39 Examples of metal–ligand bifunctional catalysts.

This journal is © The Royal Society of Chemistry 2020

Open Access Article. Published on 11 December 2019. Downloaded on 2/7/2026 6:23:02 AM.
This article is licensed under a Creative Commons Attribution-NonCommercial 3.0 Unported Licence.

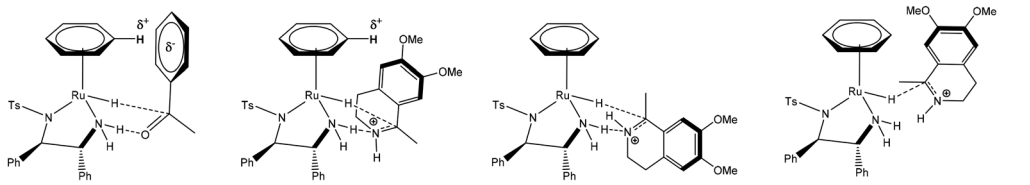

Scheme 40 Consideration of interactions in the enantioselectivity of imine and ketone reduction to afford the correct product.

6.2 ATH of imines

The significant difference between imines, alkenes and ketones is the basicity of the substrate due to the nitrogen lone pair, which in turn impacts mechanistic pathways adopted. In terms of reactive catalytic species formed in any hydrogenation protocol, one of the most important intermediates formed is the hydride species and subsequently whether hydride or proton transfer occurs first. The reaction conditions are obviously important and for Ir(III) catalysis where formic acid or iso-propanol are the source of the hydride, then for imines it is reasonable to assume that protonation of the substrate occurs first. Initial protonation significantly activates the functionality by increasing electrophilicity of the carbon hence facilitating hydride transfer which occurs subsequently.

Even with Ir(I) catalysed reduction of imines with molecular hydrogen, it seems likely that the reaction involves rapid, reversible protonation of the substrate, followed by hydride transfer from the metal. A kinetic study on the hydrogenation of C=N substrates with piano-stool ruthenium hydride complexes demonstrated that hydride transfer from the transition metal to the pre-formed iminium ion is the enantioselectivity-determining step with transfer of hydride being the rate-limiting step of the reaction.[73,100,101] This ionic hydrogenation reaction mechanism allows selective reduction of polar C=X double bonds over C=C ones, with selectivity and rate all appearing to depend on H^- transfer as the key step.[73,102]

Due to differences in basicity and susceptibility to nucleophilic attack as well as binding mode, imine hydrogenation may follow different pathways from ketonic reduction, although they do share some similarities. The control of stereochemistry in ketones is due to a favourable π/CH interaction between the hydrogen atom on the η^6-arene ligand and the aromatic ring of the substrate. The origin of enantioselection with respect to the transfer hydrogenation of imines using Noyori/CATHy catalysts is unclear. The transfer hydrogenation of imines is rather unusual as it leads to chiral amines with the opposite stereochemistry from that expected applying a similar rational. Various transition states have been proposed that could result in the correct product with the correct configuration[103,104] (Scheme 40). The suggestions are based on interactions that lead to the substrate adopting configurations that allow for transfer hydrogenation to occur yielding the enantiomeric product.

Though not conclusive, the study did confirm that the stereo-controlling effects observed in ketonic transfer hydrogenation cannot simply be superimposed onto their imine counterparts as this results in the 'wrong' product.

An outer-sphere mechanism for the iridacycle mediated hydrogenation of simple imines (Scheme 41) is initiated by chloride dissociation affording the catalytic species. The next step is hydride abstraction from the coordinated formate, releasing CO_2 and generating the hydridic species, subsequently transferring hydride-ion to the protonated imine substrate. Kinetic measurements showed that the hydrogenation rate is second order in HCO_2H concentration, first order in catalyst and zero order in imine. Using DCO_2D in place of HCO_2H yielded a k_H/k_D of 1.9, supporting Ir-hydride formation being the turnover-limiting step. Hydrogen bonding of MeOH to the formate anion stabilises the ion pair.[105]

The Ir(III)-catalysed asymmetric transfer hydrogenation of 6,7-dimethoxy-1-methyl-3,4-dihydroisoquinoline **132** (Scheme 42a) uncovered some unusual enantiomeric excess profiles for formation of the respective product amines **133** using the Ir(III) catalyst IrCp*I (*R*,*R* TsDPEN) in acetonitrile or DCM (Scheme 42) under acidic conditions.[106] In general,

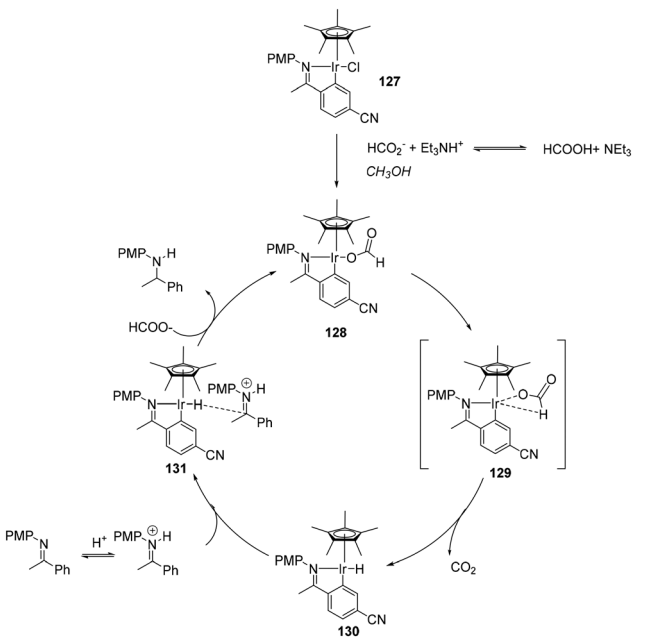

Scheme 41 ATH of acyclic imines with cyclometalated **127**.

Open Access Article. Published on 11 December 2019. Downloaded on 2/7/2026 6:23:02 AM.
This article is licensed under a Creative Commons Attribution-NonCommercial 3.0 Unported Licence.

enantioselectivity arises from differences in transition state stabilities for the two enantiomers with common kinetic orders in their rate laws. However, if the formation of the two enantiomeric products follow different rate laws then enantioselectivity can arise simply from different rates as a function of concentration of substrates.

Initially the reaction gives predominantly the (*R*)-enantiomer which then decreases significantly during further reaction. The enantioselectivity of the reduction is solvent dependent, with faster rates in dichloromethane but greater enantioselectivity in acetonitrile. The changes in ee as the reaction proceeds is a result of the rate of formation of the (*R*)-enantiomer following observed pseudo first order kinetics whereas that for the (*S*)-enantiomer is pseudo zero order. Consequently, the rate of formation of the (*R*)-enantiomer decreases as the concentration of imine decreases whereas that for (*S*)-enantiomer remains constant and so the relative rates of formation of the two enantiomers changes with time as the reaction proceeds (Scheme 42b).

Formation of the (*S*)-amine product involves rate-limiting dissociation from the catalyst **136**, step k_3 (Scheme 42c) giving rise to zero-order kinetics. The rate-limiting step for formation of the (*R*)-amine is hydride transfer **139**, supported by a H/D kinetic isotope effect, and so exhibiting normal first-order kinetics. The rate of formation of the (*S*)-amine is independent of imine concentration. Alternatively, they may be two distinct catalytic species, each responsible for the formation of the respective enantiomers.[106] Using a series of 1-fluorinated methyl-3,4-dihydroisoquinolines as substrates changes the rate-limiting step of dissociation of the (*S*)-amine product from Ir(III) k_3, so that both enantiomers are formed with first-order kinetics.[107] This results in almost complete removal of the enantioselectivity of the reduction.

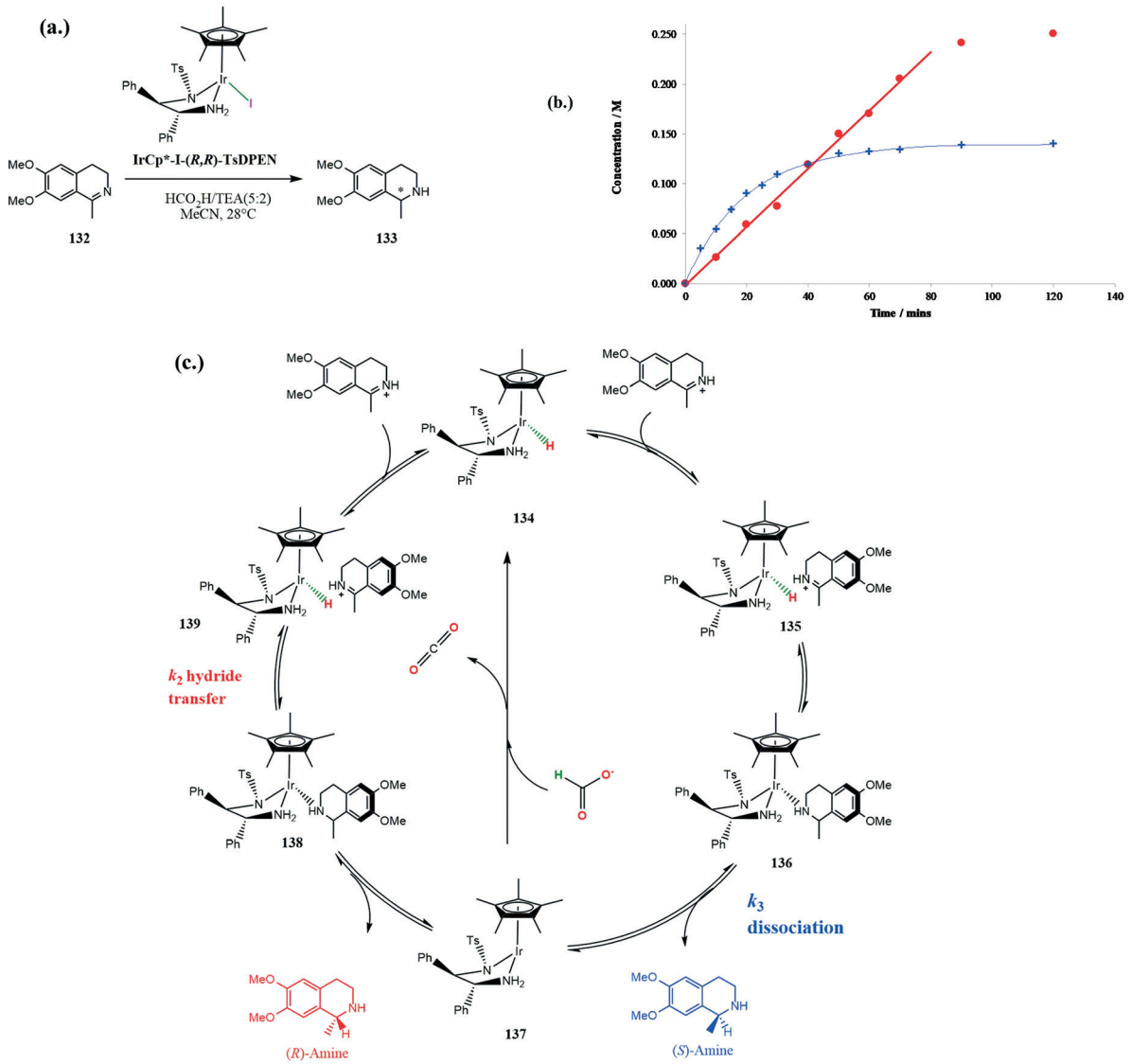

Scheme 42 Kinetic and mechanistic considerations for the formation of (*R*) and (*S*) amine.

 This journal is © The Royal Society of Chemistry 2020

Open Access Article. Published on 11 December 2019. Downloaded on 2/7/2026 6:23:02 AM.
This article is licensed under a Creative Commons Attribution-NonCommercial 3.0 Unported Licence.

It has been suggested that reduction of imines using transition metal complexes occurs through the neutral imine rather than the more reactive iminium-ion.[108] However, α-substituted imines with electron-withdrawing fluorinated groups make protonation more difficult but on the other hand enhance the electrophilicity of the imine carbon so facilitating nucleophilic attack. The α-difluoromethyl (CHF_2) 3,4-dihydroisoquinoline has a much reduced pK_a so there is little protonated species present under the reaction conditions and it is 10-fold less reactive than the α-monofluoromethyl imine in the cyclopentadienyl Ir(III) complex catalysed reduction in acetonitrile under the acidic conditions of a 5 : 2 ratio of formic acid : triethylamine. Despite a more electrophilic imine carbon the α-trifluoromethyl derivative is completely unreactive towards the cyclopentadienyl Ir(III) complex catalysed reduction, showing that the iminium ion is the reactive species.[107] It appears in this case that selectivity is almost exclusively due to the different kinetic orders for the rates of formation of the two enantiomers. Changing the ligand to *S*,*S*-TsDPEN rather than *R*,*R* inverts the kinetic orders of the rates of formation of the two enantiomeric product amines.[106,107]

6.3 ATH of ketones

A lithium mediated hydrogenation of ketones with a novel class of air-stable tridentate ferrocene-based amino-phosphine sulfonamide (f-amphamide) ligands displays excellent activity in the iridium-catalyzed asymmetric hydrogenation of aryl ketones (Scheme 43). Lithium oxide successfully promoted the hydrogenation of the carbonyl group. The catalytic cycle involves enantio-determining hydride transfer from Ir centre to the keto carbon and the H_2 activation process to yield the chiral product and regenerate the catalyst. TS1(*S*) leading to (*S*)-alcohol **142a** was found to be more stable than (*R*)-alcohol TS 1 (*R*) by 2.8 kcal mol^{-1} **142b**, leading to 98% ee. The origin of enantioselectivity is

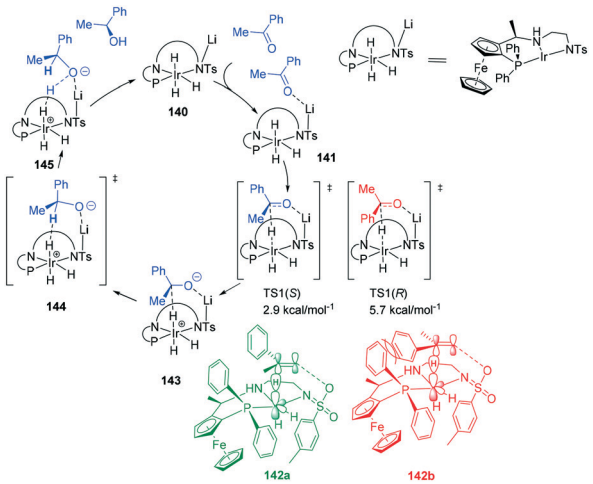

Scheme 43 Lithium assisted ATH of ketones, showing the favoured TS1(*S*) leading to 98% ee.

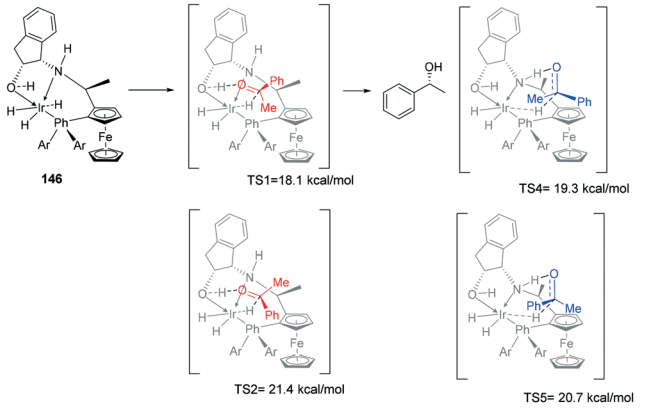

Scheme 44 Metal bifunctional complexes TS, showing the four proposed TS's with the DFT calculations predicting TS1 as being the most stable, leading to 99.9% ee.

attributed to greater steric repulsion between Ph and P of the ligand and the substrate Ph of TS1(*R*) and TS1 (*S*). This repulsion results in different bond lengths (Ir–H and C–H) in the two TS's with TS1(*R*) **142b** having longer distances than its counterpart. The repulsion leads to better overlap between the d-orbitals of the metal centre and the TS1(*S*) than TS1(*R*).[109]

Metal-bifunctional complexes provide a different approach in hydrogenation of ketones. The presence of a proton source on a ligand provides insights into the reduction process. Ferrocene-based amino-phosphine-alcohol ligands (f-amphol ligand) are efficient in the ATH of various ketones affording excellent enantioselectivities (up to 99.9% ee) and high activities (TON up to 200 000) (Scheme 44).[110] DFT calculations suggest that the hydroxyl group of f-amphol ligands plays a key role in obtaining high reactivities and excellent enantioselectivities. The f-amphol ligand contains both NH and OH labile protons. Calculated TS1 details the approach of the ketone on the *Re*-face, generating the (*R*)-alcohol whereas approach from the *Si*-face as in TS2 generates the (*S*)-alcohol. The higher free energy of TS2 of 3.3 kcal mol^{-1} highlights the kinetically unfavourable pathway. ATH at the amino side was also considered with the *Re*-face approach occurring through TS4 and *Si*-face approach occurring through TS5. The free energy of TS4 is higher than that of TS1, indicating the preferential ATH of acetophenone at the hydroxyl site. This study confirmed that the generation of (*R*)-alcohol was favoured in this catalytic protocol.[110]

7. Outlook

The use of iridium in catalysis, both homogeneous and heterogeneous, remains an exciting topic with many new developments, not only for hydrogenation/reduction reactions but for many other reactions.[111–113] The observation that enantioselectivity of some reactions can result from enantiomers being formed by different kinetic orders[106,107] highlights the importance and requirement for careful kinetic studies. The field is ripe for the application of

Open Access Article. Published on 11 December 2019. Downloaded on 2/7/2026 6:23:02 AM.
This article is licensed under a Creative Commons Attribution-NonCommercial 3.0 Unported Licence.

physical organic techniques including linear free-energy relationships and kinetic isotope effects.

Conflicts of interest

The authors declare no conflict of interest.

References

1 R. E. Gawley, *J. Org. Chem.*, 2006, **71**, 2411–2416.
2 R. P. Bell, J. E. Critchlow and M. I. Page, *J. Chem. Soc., Perkin Trans. 2*, 1974, 66–70.
3 A. Baeza and A. Pfaltz, *Chem. – Eur. J.*, 2010, **16**, 4003–4009.
4 P. J. Dyson and P. G. Jessop, *Catal. Sci. Technol.*, 2016, **6**, 3302–3316.
5 C. Reichardt and T. Welton, *Solvents and Solvent Effects in Organic Chemistry*, John Wiley & Sons, 4th edn, 2011.
6 P. S. Pregosin, *Pure Appl. Chem.*, 2009, **81**, 615–633.
7 M. I. Page and A. Williams, *Organic and Bio-organic Mechanisms*, Pearson Education Limited, Harlow, 1997, vol. 1.
8 B. Villa-Marcos, W. Tang, X. Wu and J. Xiao, *Org. Biomol. Chem.*, 2013, **11**, 6934–6939.
9 P. G. Jessop and B. Subramaniam, *Chem. Rev.*, 2007, **107**, 2666–2694.
10 Y. Schramm, F. Barrios-Landeros and A. Pfaltz, *Chem. Sci.*, 2013, **4**, 2760–2766.
11 C. Réthoré, F. Riobé, M. Fourmigué, N. Avarvari, I. Suisse and F. Agbossou-Niedercorn, *Tetrahedron: Asymmetry*, 2007, **18**, 1877–1882.
12 S. Y. Shirai, H. Nara, Y. Kayaki and T. Ikariya, *Organometallics*, 2009, **28**, 802–809.
13 L. Vaska and J. W. DiLuzio, *J. Am. Chem. Soc.*, 1961, **83**, 2784–2785.
14 R. U. Kirss, *Bull. Hist. Chem.*, 2013, **38**, 52–60.
15 A. Cadu and P. G. Andersson, *Dalton Trans.*, 2013, **42**, 14345–14356.
16 P. A. Fryzuk and M. D. MacNeil, *Organometallics*, 1983, **2**, 682–684.
17 J. A. Schrock and R. R. Osborn, *J. Am. Chem. Soc.*, 1976, **98**, 2143–2147.
18 R. H. Crabtree and G. E. Morris, *J. Organomet. Chem.*, 1977, **135**, 395–403.
19 J. W. Suggs, S. D. Cox, R. H. Crabtree and J. M. Quirk, *Tetrahedron Lett.*, 1981, **22**, 303–306.
20 G. Stork and D. E. Kahne, *J. Am. Chem. Soc.*, 1983, **105**, 1072–1073.
21 R. H. Crabtree and M. W. Davis, *Organometallics*, 1983, **2**, 681–682.
22 M. W. Davis and R. H. Crabtree, *J. Org. Chem.*, 1986, **51**, 2655–2661.
23 A. G. Schultz, P. J. McCloskey and J. J. Court, *J. Am. Chem. Soc.*, 1987, **109**, 6493–6502.
24 H. Takaya, T. Ohta, N. Sayo, H. Kumobayashi, S. Akutagawa, S. Inoue, I. Kasahara and R. Noyori, *J. Am. Chem. Soc.*, 1987, **109**, 1596–1597.
25 R. Sablong and J. A. Osborn, *Tetrahedron Lett.*, 1996, **37**, 4937–4940.
26 F. Spindler, B. Pugin and H.-U. Blaser, *Angew. Chem., Int. Ed. Engl.*, 1990, **29**, 558–559.
27 C. Bianchini, P. Barbaro, G. Scapacci, E. Farnetti and M. Graziani, *Organometallics*, 1998, **17**, 3308–3310.
28 D. Xiao and X. Zhang, *Angew. Chem., Int. Ed.*, 2001, **40**, 3425–3428.
29 K. Morimoto, T. Nakajima and N. Achiwa, *Chem. Pharm. Bull.*, 1994, **42**, 1951–1953.
30 H. U. Blaser, B. Pugin, F. Spindler, E. Mejía and A. Togni, Josiphos Ligands: From Discovery to Technical Applications, *Top. Catal.*, 2002, **19**, 3, DOI: 10.1023/A:1013832630565.
31 R. Dorta, D. Broggini, R. Stoop, H. Rüegger, F. Spindler and A. Togni, *Chem. – Eur. J.*, 2004, **10**, 267–278.
32 K. Ziegler, E. Holzkamp, H. Breil and H. Martin, *Angew. Chem.*, 1955, **67**, 426–426.
33 S. M. Lu, Y. Q. Wang, X. W. Han and Y. G. Zhou, *Angew. Chem., Int. Ed.*, 2006, **45**, 2260–2263.
34 T. Morimoto, N. Nakajima and K. Achiwa, *Synlett*, 1995, **7**, 748–750.
35 C. J. Hou, Y. H. Wang, Z. Zheng, J. Xu and X. P. Hu, *Org. Lett.*, 2012, **14**, 3554–3557.
36 W. B. Wang, S. M. Lu, P. Y. Yang, X. W. Han and Y. G. Zhou, *J. Am. Chem. Soc.*, 2003, **125**, 10536–10537.
37 S. M. Lu, X. W. Han and Y. G. Zhou, *Adv. Synth. Catal.*, 2004, **346**, 909–912.
38 G. Hou, R. Tao, Y. Sun, X. Zhang and F. Gosselin, *J. Am. Chem. Soc.*, 2010, **132**, 2124–2125.
39 K. Gao, C. Bin Yu, W. Li, Y. G. Zhou and X. Zhang, *Chem. Commun.*, 2011, **47**, 7845–7847.
40 T. Kazuhide, O. Jun-ichiro, Y. Tsuneaki and K. Yasutaka, *Chem. Lett.*, 1995, 955–956.
41 Y. Chi, Y. G. Zhou and X. Zhang, *J. Org. Chem.*, 2003, **68**, 4120–4122.
42 H. L. Kim, L. Xu, L. Feng, Q. H. Fan, L. L. Fuk, W. H. Lo and A. S. C. Chan, *Adv. Synth. Catal.*, 2005, **347**, 1755–1758.
43 W. J. Tang, S. F. Zhu, L. J. Xu, Q. L. Zhou, Q. H. Fan, H. F. Zhou, K. Lam and A. S. C. Chan, *Chem. Commun.*, 2007, 613–615.
44 W. Tang, L. Xu, Q. H. Fan, J. Wang, B. Fan, Z. Zhou, K. H. Lam and A. S. C. Chan, *Angew. Chem., Int. Ed.*, 2009, **48**, 9135–9138.
45 W. Tang, Y. Sun, X. Lijin, T. Wang, Q. Fan, K. H. Lam and A. S. C. Chan, *Org. Biomol. Chem.*, 2010, **8**, 3464–3471.
46 X. Bin Jiang, A. J. Minnaard, B. Hessen, B. L. Feringa, A. L. L. Duchateau, J. G. O. Andrien, J. A. F. Boogers and J. G. De Vries, *Org. Lett.*, 2003, **5**, 1503–1506.
47 A. Pfaltz, *Acta Chem. Scand.*, 1996, **50**, 189–194.
48 P. von Matt and A. Pfaltz, *Angew. Chem., Int. Ed. Engl.*, 1993, **32**, 566–568.
49 P. von Matt, O. Loiseleur, G. Koch, A. Pfaltz, C. Lefeber, T. Feucht and G. Helmchen, *Tetrahedron: Asymmetry*, 1994, **5**, 573–584.
50 D. Müller, G. Umbricht, B. Weber and A. Pfaltz, *Helv. Chim. Acta*, 1991, **74**, 232–240.

 This journal is © The Royal Society of Chemistry 2020

Open Access Article. Published on 11 December 2019. Downloaded on 2/7/2026 6:23:02 AM.
This article is licensed under a Creative Commons Attribution-NonCommercial 3.0 Unported Licence.

51 S. Vargas, M. Rubio, A. Suárez and A. Pizzano, *Tetrahedron Lett.*, 2005, **46**, 2049–2052.
52 P. Schnider, G. Koch, R. Prétôt, G. Wang, F. M. Bohnen, C. Krüger and A. Pfaltz, *Chem. – Eur. J.*, 1997, **3**, 887–892.
53 C. Blanc, F. Agbossou-Niedercorn and G. Nowogrocki, *Tetrahedron: Asymmetry*, 2004, **15**, 2159–2163.
54 A. Lightfoot, P. Schnider and A. Pfaltz, *Angew. Chem., Int. Ed.*, 1998, **37**, 2897–2899.
55 A. Triforiova, J. S. Diesen, C. J. Chapman and P. G. Andersson, *Org. Lett.*, 2004, **6**, 3825–3827.
56 S. Kainz, A. Brinkmann, W. Leitner and A. Pfaltz, *J. Am. Chem. Soc.*, 1999, **121**, 6421–6429.
57 M. Solinas, A. Pfaltz, P. G. Cozzi and W. Leitner, *J. Am. Chem. Soc.*, 2004, **126**, 16142–16147.
58 S. Vargas, M. Rubio, A. Suárez, D. Del Río, E. Álvarez and A. Pizzano, *Organometallics*, 2006, **25**, 961–973.
59 N. Mršić, A. J. Minnaard, B. L. Feringa and J. G. De Vries, *J. Am. Chem. Soc.*, 2009, **131**, 8358–8359.
60 A. Baeza and A. Pfaltz, *Chem. – Eur. J.*, 2009, **15**, 2266–2269.
61 M. N. Cheemala and P. Knochel, *Org. Lett.*, 2007, **9**, 3089–3092.
62 S. F. Zhu, J. B. Xie, Y. Z. Zhang, S. Li and Q. L. Zhou, *J. Am. Chem. Soc.*, 2006, **128**, 12886–12891.
63 Z. Han, Z. Wang, X. Zhang and K. Ding, *Angew. Chem., Int. Ed.*, 2009, **48**, 5345–5349.
64 A. Iimuro, K. Yamaji, S. Kandula, T. Nagano, Y. Kita and K. Mashima, *Angew. Chem., Int. Ed.*, 2013, **52**, 2046–2050.
65 H. Tadaoka, D. Cartigny, T. Nagano, T. Gosavi, T. Ayad, J. P. Genêt, T. Ohshima, V. Ratovelomanana-Vidal and K. Mashima, *Chem. – Eur. J.*, 2009, **15**, 9990–9994.
66 Z. W. Li, T. L. Wang, Y. M. He, Z. J. Wang, Q. H. Fan, J. Pan and L. J. Xu, *Org. Lett.*, 2008, **10**, 5265–5268.
67 C. Tian, L. Gong and E. Meggers, *Chem. Commun.*, 2016, **52**, 4207–4210.
68 G. J. Kubas, *J. Organomet. Chem.*, 2014, **751**, 33–49.
69 M. Ito and T. Ikariya, *Chem. Commun.*, 2007, 5134–5142.
70 M. Peruzzini and R. Poli, *Recent Advances in Hydride Chemistry*, Elsevier SA, Amsterdam, 2001.
71 O. Eisenstein and R. H. Crabtree, *New J. Chem.*, 2013, **37**, 21–27.
72 K. H. Hopmann and A. Bayer, *Organometallics*, 2011, **30**, 2483–2497.
73 R. M. Bullock, *Chem. – Eur. J.*, 2004, **10**, 2366–2374.
74 N. Uematsu, A. Fujii, S. Hashiguchi, T. Ikariya and R. Noyori, *J. Am. Chem. Soc.*, 1996, **118**, 4916–4917.
75 J. B. Johnson and J. E. Bäckvall, *J. Org. Chem.*, 2003, **68**, 7681–7684.
76 Y. Huang, S. Liu, Y. Liu, Y. Chen, M. Weisel, R. T. Williamson, I. W. Davies and X. Zhang, *Tetrahedron*, 2018, **74**, 2182–2190.
77 J. S. M. Samec, A. H. Éll and J. E. Bäckvall, *Chem. Commun.*, 2004, 2748–2749.
78 A. Comas-Vives, G. Ujaque and A. Lledós, *Inner- and Outer-Sphere Hydrogenation Mechanisms: A Computational Perspective*, Elsevier Inc., 2010, vol. 62.
79 B. Villa-Marcos, C. Li, K. R. Mulholland, P. J. Hogan and J. Xiao, *Molecules*, 2010, **15**, 2453–2472.
80 G. Koch, G. C. Lloyd-Jones, O. Loiseleur, A. Pfaltz, R. Prétôt, S. Schaffner, P. Schnider and P. von Matt, *Recl. Trav. Chim. Pays-Bas*, 1995, **114**, 206–210.
81 M. Martín, E. Sola, S. Tejero, J. A. López and L. A. Oro, *Chem. – Eur. J.*, 2006, **12**, 4043–4056.
82 D. Zhao, L. Candish, D. Paul and F. Glorius, *ACS Catal.*, 2016, **6**, 5978–5988.
83 S. Gülcemal, A. G. Gökçe and B. Çetinkaya, *Inorg. Chem.*, 2013, **52**, 10601–10609.
84 S. Díez-González, N. Marion and S. P. Nolan, *Chem. Rev.*, 2009, **109**, 3612–3676.
85 C. Diez and U. Nagel, *Appl. Organomet. Chem.*, 2010, **24**, 509–516.
86 F. Aznarez, M. Iglesias, A. Hepp, B. Veit, P. J. Sanz Miguel, L. A. Oro, G. X. Jin and F. E. Hahn, *Eur. J. Inorg. Chem.*, 2016, **2016**, 4598–4603.
87 M. N. Hopkinson, C. Richter, M. Schedler and F. Glorius, *Nature*, 2014, **510**, 485–496.
88 H. Chiyojima and S. Sakaguchi, *Tetrahedron Lett.*, 2011, **52**, 6788–6791.
89 Y. Li, M. Lei, W. Yuan, E. Meggers and L. Gong, *Chem. Commun.*, 2017, **53**, 8089–8092.
90 G. E. Dobereiner, A. Nova, N. D. Schley, N. Hazari, S. J. Miller, O. Eisenstein, R. H. Crabtree and I. C. Gerhardt, *J. Am. Chem. Soc.*, 2011, **133**(19), 7547–7562.
91 J. M. Hayes, E. Deydier, G. Ujaque, A. Lledós, R. Malacea-Kabbara, E. Manoury, S. Vincendeau and R. Poli, *ACS Catal.*, 2015, **5**, 4368–4376.
92 M. Iglesias and L. A. Oro, *Chem. Soc. Rev.*, 2018, **47**, 2772–2808.
93 N. García, E. A. Jaseer, J. Munarriz, P. J. Sanz Miguel, V. Polo, M. Iglesias and L. A. Oro, *Eur. J. Inorg. Chem.*, 2015, **2015**, 4388–4395.
94 J. W. Handgraaf, J. N. H. Reek and E. J. Meijer, *Organometallics*, 2003, **22**, 3150–3157.
95 O. Pàmies and J. E. Bäckvall, *Chem. – Eur. J.*, 2001, **7**, 5052–5058.
96 R. Noyori and S. Hashiguchi, *Acc. Chem. Res.*, 1997, **30**, 97–102.
97 R. Soni, F. K. Cheung, G. C. Clarkson, J. E. D. Martins, M. A. Graham and M. Wills, *Org. Biomol. Chem.*, 2011, **9**, 3290–3294.
98 C. A. Sandoval, T. Ohkuma, K. Muñiz and R. Noyori, *J. Am. Chem. Soc.*, 2003, **125**, 13490–13503.
99 W. Wu, S. Liu, M. Duan, X. Tan, C. Chen, Y. Xie, Y. Lan, X. Q. Dong and X. Zhang, *Org. Lett.*, 2016, **18**, 2938–2941.
100 N. Onishi, M. Z. Ertem, S. Xu, A. Tsurusaki, Y. Manaka, J. T. Muckerman, E. Fujita and Y. Himeda, *Catal. Sci. Technol.*, 2016, **6**, 988–992.
101 V. Herrera, B. Muñoz, V. Landaeta and N. Canudas, *J. Mol. Catal. A: Chem.*, 2001, **174**, 141–149.
102 M. P. Magee and J. R. Norton, *J. Am. Chem. Soc.*, 2001, **123**, 1778–1779.
103 J. E. D. Martins, G. J. Clarkson and M. Wills, *Org. Lett.*, 2009, **11**, 847–850.
104 R. Soni, K. E. Jolley, S. Gosiewska, G. J. Clarkson, Z. Fang, T. H. Hall, B. N. Treloar, R. C. Knighton and M. Wills, *Organometallics*, 2018, **37**, 48–64.

Open Access Article. Published on 11 December 2019. Downloaded on 2/7/2026 6:23:02 AM.
This article is licensed under a Creative Commons Attribution-NonCommercial 3.0 Unported Licence.

105 C. Wang and J. Xiao, *Chem. Commun.*, 2017, **53**, 3399–3411.
106 M. J. Stirling, G. Sweeney, K. Macrory, A. J. Blacker and M. I. Page, *Org. Biomol. Chem.*, 2016, **14**, 3614–3622.
107 J. M. Mwansa, M. J. Stirling and M. I. Page, *Pure Appl. Chem.*, DOI: 10.1515/pac-2019-0222.
108 D. G. Blackmond, M. Ropic and M. Stefinovic, *Org. Process Res. Dev.*, 2006, **10**, 457–463.
109 Z. Liang, T. Yang, G. Gu, L. Dang and X. Zhang, *Chin. J. Chem.*, 2018, **36**, 851–856.
110 J. Yu, M. Duan, W. Wu, X. Qi, P. Xue, Y. Lan, X. Q. Dong and X. Zhang, *Chem. – Eur. J.*, 2017, **23**, 970–975.
111 Q. Cheng, H. F. Tu, C. Zheng, J. P. Qu, G. Helmchen and S. L. You, *Chem. Rev.*, 2019, **119**, 1855–1969.
112 M. M. Zhang, Y. N. Wang, B. C. Wang, X. W. Chen, L. Q. Lu and W. J. Xiao, *Nat. Commun.*, 2019, **10**, 1–9.
113 A. G. Schafer and S. B. Blakey, *Chem. Soc. Rev.*, 2015, **44**, 5969–5980.

 This journal is © The Royal Society of Chemistry 2020